Guilherme Balieiro Gomes

Quantum Dissipation and Decoherence in Neutrino Oscillations

Dissipação e Descoerência Quântica em Oscilação de Neutrinos

CAMPINAS
2014

Universidade Estadual de Campinas

Instituto de Física "Gleb Wataghin"

Guilherme Balieiro Gomes

Quantum Dissipation and Decoherence in Neutrino Oscillations

Dissipação e Descoerência Quântica em Oscilação de Neutrinos

Dissertation presented to the Institute of Physics "Gleb Wataghin" of the University of Campinas in partial fulfillment of the requirements for the degree of Master in Physics.

Dissertação apresentada ao Instituto de Física "Gleb Wataghin" da Universidade Estadual de Campinas como parte dos requisitos exigidos para a obtenção do título de Mestre em Física.

Orientador: Prof. Dr. Marcelo Moraes Guzzo

Este exemplar corresponde à versão final da dissertação defendida pelo aluno Guilherme Balieiro Gomes e orientada pelo Prof. Dr. Marcelo Moraes Guzzo.

Assinatura do Orientador

Campinas
2014

Ficha catalográfica
Universidade Estadual de Campinas
Biblioteca do Instituto de Física Gleb Wataghin
Valkíria Succi Vicente - CRB 8/5398

B198q

Balieiro Gomes, Guilherme, 1989-
Quantum dissipation and decoherence in neutrino oscillations / Guilherme Balieiro Gomes. – Campinas, SP : [s.n.], 2014.

Orientador: Marcelo Moraes Guzzo.
Dissertação (mestrado) – Universidade Estadual de Campinas, Instituto de Física Gleb Wataghin.

1. Neutrinos. I. Guzzo, Marcelo Moraes,1963-. II. Universidade Estadual de Campinas. Instituto de Física Gleb Wataghin. III. Título.

Informações para Biblioteca Digital

Título em outro idioma: Dissipação e descoerência quântica em oscilação de neutrinos
Palavras-chave em inglês:
Neutrinos
Área de concentração: Física
Titulação: Mestre em Física
Banca examinadora:
Marcelo Moraes Guzzo [Orientador]
Celso Chikahiro Nishi
Marcio José Menon
Data de defesa: 29-05-2014
Programa de Pós-Graduação: Física

MEMBROS DA COMISSÃO JULGADORA DA DISSERTAÇÃO DE MESTRADO DE **GUILHERME BALIEIRO GOMES - RA 081526** APRESENTADA E APROVADA AO INSTITUTO DE FÍSICA "GLEB WATAGHIN", DA UNIVERSIDADE ESTADUAL DE CAMPINAS, EM 29 / 05 / 2014.

COMISSÃO JULGADORA:

Prof. Dr. Marcelo Moraes Guzzo - Orientador do Candidato
DRCC/IFGW/UNICAMP

Prof. Dr. Celso Chikahiro Nishi – CMCC/UFABC

Prof. Dr. Marcio José Menon – DRCC/IFGW/UNICAMP

Abstract

In this dissertation, using Quantum Open Systems we analyze data from KamLAND by using a model that considers neutrino oscillation in two families with the inclusion of the decoherence effect.

We review important concepts of usual Quantum Mechanics, such as the superposition principle, coherence, and the measurement problem. We also review the density matrix formalism and we use it to present the theory of Quantum Open Systems, which gives the Lindblad - Kossakowski equation.

Vaccum neutrino oscillations are studied using the density matrix formalism, and then the lindblad - Kossakowski equation is used to obtain new equations for the neutrino oscillations in two families, in which we see the inclusion of the decoherence effect

Then, we use a χ^2 Test to find limits for the usual oscillation parameters and also for the decoherence parameter which we call γ.

We find evidence in favor of the inclusion of the decoherence effect, since the analysis shows that a zero value for the decoherence parameter γ is excluded in 68.27% C.L.

Resumo

Nessa dissertação, utilizando a Mecânica Quântica de Sistemas Abertos, analisamos dados de KamLAND utilizando um modelo que considera oscilação de neutrinos em duas famílias incluindo-se o efeito de descoerência quântica.

Revisamos conceitos importantes de Mecânica Quântica usual, como o princípio de superposição, coerência quântica, e o problema da medida. Revemos também o formalismo de matriz de densidade e o utilizamos para apresentar a Mecânica Quântica de Sistemas Abertos, da qual obtemos a equação de Lindblad - Kossakowski.

Oscilação de neutrinos no vácuo são revisadas utilizando o formalismo de matriz de densidade, e então a equação de Lindblad - Kossakowski é usada para obtermos novas equações para oscilação de neutrinos em duas famílias, onde vemos a inclusão do efeito de descoerência quântica.

Então, usamos um teste de χ^2 para obter limites para os parâmetros usuais de oscilação de neutrinos e também para o parâmetro de descoerência, que chamamos de γ.

Encontramos evidências em favor da inclusão do efeito de descoerência quântica , uma vez que nossa análise mostrou que o valor $\gamma = 0$ está excluído em 68,27%C.L.

Contents

Agradecimentos

Inicialmente quero agradecer aos meus pais, Marcelo e Áurea, e também à minha irmã, Caroline, por todo o apoio, amor e paciência durante esses mais de seis anos de Unicamp. Por sempre terem me escutado, tanto nos momentos de crise e de dúvida, quanto nos momentos em que tudo corria bem. Embora nem sempre eu tenha voltado para casa o quanto vocês queriam, e nem sempre eu pude ficar com vocês por mais tempo, saibam que eu amo muito vocês.

Agradeço a todos os meus amigos que me acompanharam nesse período aqui, seja durante a graduação, seja durante o mestrado. Em especial, destaco Leandro, Astro, Yuzo, Hideki, Caião, Fabão, Leônidas, Allan, Diego, Naty, Mai, Adriano, Bruno, Rosa, Thaís, Joe, Paola, Marcos, Gira, César e inúmeros outros que tornaram muito mais agradável meu tempo nesta universidade.

Agradeço ao Leandro pelas várias horas de estudo que foram importantes durante esse mestrado, além das inúmeras boas conversas que vêm desde antes de entrarmos na Unicamp.

Agradeço também a todos os meus amigos de Marília, principalmente ao Fabrício, Zé, Wisk, Lester, Tiago e Danilo, que sem dúvida foram muito importantes nos momentos não acadêmicos.

Agradeço a toda a minha família, mas particularmente à minha tia Marlene, com quem eu moro há mais de seis anos, e que é uma segunda mãe pra mim, sendo sempre uma ótima companhia, sempre interessada em ouvir sobre o que eu estava estudando ou sobre o que mais eu quisesse conversar.

Agradeço ao Prof. Marcelo Guzzo por ter sido um excelente orientador desde minha iniciação científica, sendo sempre uma grande fonte de inspiração pra mim, por seu grande conhecimento e inteligência, por sua paixão pela física que sempre transparece quando conversamos, e também como exemplo em outras áreas, sempre muito correto e preocupado com a formação completa de seus alunos, não somente em física.

Agradeço também a todos os demais professores que contribuíram para minha formação, e também aos diversos funcionários da Unicamp que me auxiliaram direta ou indiretamente, e que assim, foram parte importante desse meu período como aluno da Unicamp.

Agradeço ao César, não só pelas agradabilíssimas conversas sobre filosofia e os mais variados assuntos, mas também pelas ajudas nas disciplinas, na preparação para o Pré-Requisito, e em muitas outras atividades acadêmicas. Agradeço também ao Mateus Carneiro pela ajuda com o Fortran, ao Felipe Penha pela ajuda com as curvas de Confidence Level, ao Pedro Pasquini pela ajuda na preparação para o Pré-Requisito e com outras dúvidas, ao Zavanin, que sempre esteve disposto a me ajudar com dúvidas em geral, ao Yuzo pela ajuda com o Latex, ao Adriano e ao Bruno pela ajuda com outros gráficos.

Agradeço ao Roberto pelas diversas discussões, ajudas, explicações, sugestões de referências,

e inúmeras outras ajudas que foram essenciais para que este trabalho fosse realizado. Agradeço também ao Prof. Pedro Holanda, que também deu contribuições essenciais, tanto pelos programas que ele disponibilizou, quanto por diversas ideias e sugestões que foram importantíssimas para a obtenção e compreensão dos resultados.

Agradeço à Unicamp pela possibilidade de estudar aqui, e à CAPES pela bolsa de mestrado.

List of Figures

List of Tables

Chapter 1

Introduction

It is well known that Quantum Mechanics can be used to describe successfully a variety of systems, and that its applicability has increased a lot since it was created. Nevertheless, in spite of its success, the theory of Quantum Mechanics has its limitations, and so, developing and testing extensions to Quantum Mechanics and other Quantum theories is very important to the development of science and to understand the universe.

An example of a limitation of usual Quantum Mechanics is that it does not consider relativistic effects. This problem served as motivation for several studies, which led to the creation of important theories such as the Quantum Electrodynamics (QED), a theory that has a great success in terms of being confirmed by experiments, and because of that inspired the creation of many other theories.

In this dissertation, we are going to consider a different limitation of usual Quantum Mechanics: the fact that it uses the assumption that the studied system is isolated. The theory of Quantum Open Systems was one of the theories created to deal with this issue [2,16]. In this theory, the system of interest is no longer considered isolated, but is regarded as having a coupling with the enviroment, and such coupling has important consequences, since we are dealing with quantum systems.

An important feature of quantum theories is the existence of the superposition principle, which makes possible the description of a given state in terms of a linear superposition of other states. This is precisely the case for the neutrino, since a neutrino flavor state may be desbribed as a coherent superposition of mass states.

Neutrinos are spin 1/2 particles, with null electric charge and null color charge, which means that they only interact by the weak interaction [17]. Because of that, they have a great capacity of penetration, what makes the neutrinos a powerfull tool to study several aspects of nature, but also makes their detection very difficult.

A direct consequence of the description of the neutrino as a superposition of states is the phenomenon of neutrino oscillations [6,18].

When the neutrino oscillations were created, they arised as a possible solution for the solar neutrino problem [5], but they require the assumption that the neutrinos have mass, which does not agree with the minimal version of the Standard Model of particle physics [19].

Since it was created, a lot of experiments were constucted to verify the existence of neutrino oscillations [20 - 22], and the confirmation came from neutrinos of many different sources, like solar

neutrinos, atmospheric neutrinos, accelerator neutrinos and reactor neutrinos, and now the idea that neutrinos have mass is widely accepted.

In general, the study of vacuum neutrino oscillations is made in the framework of usual Quantum Mechanics, which considers the system of neutrinos as isolated. In this dissertation we will do a different kind of analysis, in the framework of Quantum Open Systems, considering that the subsystem of interest has a coupling with the enviroment.

As we will see, the coupling with the enviroment will act changing the superposition of states, eliminating the coherence, similarly to what we have when a measurement is made in a quantum system. We see then, that this coupling generates a decoherence effect.

The first goal of this dissertation is to verify how the theory of Quantum Open Systems modify the probabilities of neutrino oscillations by means of the decoherence effect. We know that Quantum Mechanics in its usual formulation is the theory used to build the usual model for neutrino oscillations, and that this model accounts for experimental data. Nevertheless, our motivation is linked to the possibility of testing non-standard effectcs in order to try to find a better fit for experimental data and maybe also to serve as a test for Quantum Mechanics itself. The description of these effects, even if they end up being second order effects, is important to the comprehension of the physical features of all physical systems. This should also be the case for the neutrinos, and so, we will study how the neutrinos behave with the inclusion of new characteristics.

Then, after having the different expressions for the probabilities, we will confront them with experimental data from KamLAND, a reactor neutrino experiment located in Japan, and we will obtain limits for the parameters used to describe the neutrino oscillations with decoherence.

To do so, in Chapter 2 we will review the concepts of quantum superposition, decoherence, and the measurement problem, showing and example of how a coupling between the system of interest and the measurement instrument could be used to work on the measurement problem. We will also study the formalism of Density Matrix and use it to study the main features of Quantum Open Systems and to develop an equation for the time evolution of a subsystem of interest which has a coupling with the enviroment. This equation is known as the Lindblad - Kossakowski equation.

In Chapter 3 we will study the neutrino oscillations in the density matrix formalism, and we will apply the results obtained in Chapter 2, getting then the modified expressions for the neutrino oscillations with decoherence. We study two different cases, and find two different expressions for the neutrino oscillation. These two expressions are then analyzed, to verify their physical properties

In Chapter 4 we make a brief review of neutrino experiments in general and mainly of the KamLAND experiment, since it was the source of the data used for the analysis in this work. We also present the methodology of the analysis of the data, defining the model used for the χ^2 Test and explaining how the program we used test the models for neutrino oscillations using the data from KamLAND.

In Chapter 5 we show the final results of the analysis, giving limits for the parameters that our model use to describe the neutrino oscillations, and we also show interpretations of these results, by means of graphs that show the differences of the oscillation pattern with and without the inclusion of the decoherence effect.

In this work, we consider a theory that doesn't use the assumption that the system of interest is isolated because it seems more realistic, and we want to verify in a phenomenological way if

this is a more realistic model, that would contribute to the understanding of important physical systems.

We also wish to make a good overview of the subject, from its relation to basic concepts of Quantum Mechanics, to its consequences in the confrontation with experimental data.

Chapter 2

Quantum Open Systems

In this chapter, we will present concepts and ideas related to dissipative effects in Quantum Mechanics. We will begin with a review of superposition effects in closed systems, and how the superposition of states cease to exist when a measurement is made in the system. This is the measurement problem in Quantum Mechanics, which will be better defined in section 2.2.

In the way it is postulated, the measurement process is able to suppress the quantum superpositions, and we can deal with this problem imposing that the subsystem of interest is in constant interaction with the measurement instrument. In this way, the system and the measurement instrument form correlated states, and therefore, if we want to get information from the subsystem of interest, some of its local features may be lost, and that may be the case for the quantum superpositions, as will be shown more clearly in section 2.2.

We will then consider a global state, in which there is a coupling between the subsystem of interest and the enviroment around it, and this enviroment will be seen as a continuously acting measurement instrument, and the decoherence process will be responsible for dinamically removing the quantum superpositions in the subsystem. So, the decoherence effect will be naturally included in the description of the subsystem of interest.

There are cases in which we can create a model for the eviroment that interacts with the subsystem of interest, but in many cases, the quantum states of the enviroment are not important or are very difficult to be described. Nevertheless, since the real nature of the enviroment is not known, and our interest is only on the subsystem which is under the dissipative process, we will treat the enviroment in a phenomenological way, assuming total ignorance about it, and considering only its effects on the subsystem of interest, which will then be evolved in time. This way, it will be possible to study every possible effect, as will be seen in the next chapters.

In this chapter, we will see how to obtain information from the subsystem of interest given a global state, and how to evolve this subsystem in time. In doing so, we will obtain the equation of Lindblad - Kossakowski, that rules the dynamics of the subsystem of interest. It has the form of a master equation, when we assume that the coupling between the subsystem of interest and the enviroment is very weak. In the literature, the case studied and applied in this dissertation is known as weak-coupling limit [3]. At last, to make the states become increasingly mixed, and not the opposite, it will be imposed the maximization of the von Neumann entropy, and as a consequence, we will get a condition for the quantum dissipator that, in adition to other concepts

that will be studied later, will restrict the phenomenological parameters used to describe the quantum dissipation.

2.1 Quantum Superposition

A good understanding of the meaning of quantum superposition is very important, mainly because it is a feature that make the distintion between what we usually call quantum physics and classical physics. Superpositions in classical physics can be considered trivial and very intuitive, but that is not the case for superpositions in quantum physics, since they are one of its main aspects, and they appear in the most intriguing effects we know, and so are certaily not intuitive. Many discussions about the meaning of quantum superpositions can be found in the literature [23 - 25].

The superposition principle can always be applied when we have a basis of quantum states. With this basis, it is possible to write new quantum states, doing a linear superposition of the states. Considering a two-level system, for example, with the basis of eigenstates $\{|\psi_1\rangle, \psi_2\rangle\}$ we can always write a new state as:

$$|\psi\rangle = c_1|\psi_1\rangle + c_2|\psi_2\rangle \tag{2.1.1}$$

Where c_1 and c_2 are complex numbers, $|c_1|^2+|c_2|^2= 1$ for normalized states. Also, if $|\psi_1(t)\rangle$ and $|\psi_2(t)\rangle$ are solutions of the Schroedinger equation, then $|\psi(t)\rangle$ is also a solution, with $|c_1(t)|^2+|c_2(t)|^2= 1$ where $c_1(t)$ and $c_2(t)$ are the probability amplitudes.

The superposition principle is directly related to the issue of measuring physical properties of a system. As we know from Quantum Mechanics, the quantity measured must be an observable, and the possible outcomes of the measurement are all of its eigenvalues. So, treating the measurement as a probability of obtaining a given eigenvalue, we can see how the quantum superposition of states determines the behavior of the probability. To do so, let's consider again the two-level system we already described, and assume that there is an observable X with eigenvalues x_n and normalized eigenvectors $|x_n\rangle$ and that we want to know the probability of measuring the eigenvalue x_n when the state prepared is (2.1), we have

$$\begin{aligned} P(x_n) &= |\langle x_n|\psi\rangle|^2 \\ &= |c_1\langle x_n|\psi_1\rangle + c_2\langle x_n|\psi_2\rangle|^2 \\ &= |c_1|^2|\langle x_n|\psi_1\rangle|^2 + |c_2|^2|\langle x_n|\psi_2\rangle|^2 + 2\mathcal{R}c_1c_2^*\langle x_n|\psi_1\rangle\langle x_n|\psi_2\rangle^* \end{aligned} \tag{2.1.2}$$

in the last line of the equation above we see the term which shows that the state $|\psi\rangle$ is not just a statistical mixture, and that the probability not only gives information about the quantum interference (or coherence) between the superposed states, but also depends on it to make the correct quantum prediction [15].

2.2 Observables and the Measurement Process

In the previous section we discussed that examining the quantum probabilities we are dealing with, is a way of examining the possible outcomes of a given physical phenomenon. And, as we said before, we want to know what to expect of a system when it is subjected to a given measurement. Now, we will discuss the effect of the measurement in the subsystem of interest, and to do so, we'll keep using the example of the previous section. Considering the operator X that belongs to a Hilbert space, we can always write it as

$$X = \sum_n x_n |x_n\rangle\langle x_n| \tag{2.2.1}$$

Where we can define the operator of projection $P_n = |x_n\rangle\langle x_n|$ whith $\sum P_n = \mathbb{1}$ and $\{|x_n\rangle\}$ a normalized basis. So, a state that is initially prepared as (2.1.1), after the measurement goes "immediately" to the state $|x_n\rangle$, which means that, when we measure x_n we have

$$|\psi\rangle \overset{x_n}{\Rightarrow} |x_n\rangle \tag{2.2.2}$$

This is the so called wave function collapse.

As it was presented here, it still needs the temporal dynamic aspect, and we will see that there are some problems regarding the time duration of the collapse, which we postulated before as happening "immediately" after the measurement, and some problems regarding the real meaning of a measurement.

To complete the measurement events, we will assume that the state (2.1.1) can be described in terms of the basis $\{|x_n\rangle\}$, and is written as

$$|\psi\rangle = \sum_n a_n |x_n\rangle \tag{2.2.3}$$

Using the Schroedinger Equation to evolve in time the state above, we have:

$$|\psi(t)\rangle = \sum_n a_n(t) |x_n\rangle \tag{2.2.4}$$

We can view the system as evolving in time from $t = 0 \rightarrow |\psi(0)\rangle$ to $t = t_0 \rightarrow |\psi(t_0)\rangle$ when an instrument represented by the operator X measures the value x_n, and then, for $t > t_0$ the system is in the state $|x_n\rangle$.

It is necessary to discuss carefully how all the superpositions $|\psi(t)\rangle$ are suppressed at the instant t_0 when the collapse supposely happens. This is one of the questions that form the so called measurement problem and it is still an open question.

In the literature there are several works, with different views, which suggest modifications to Quantum Mechanics to explain the details of the real physical mecanisms of the process in which the wavefunction of a state of the type (2.2.4) collapses to $|x_n\rangle$ [4,26 - 28].

We will use an approach that takes into account the interaction between the system of interest that will be measured and the measurement instrument. Such interaction is responsible for limiting our knowledge of the quantum superposition of states. To do that, we will need to change the definition of an observable, since the one we used before wasn't very realistic, and, in a more

general view, an observable must be obtained from its correspondent interaction Hamiltonian and from the initial states of the measurement instrument. Such interaction must be diagonal in the basis of the measurement system, which means that these operators act only on the space of the measurement system. To clarify how to apply this idea, we can consider a state composed by the system of interest and the possible states of the measurement system. The initial state can be written as [15]

$$\sum a_n(t)|x_n\rangle \ |\Phi_n\rangle \tag{2.2.5}$$

And the Hamiltonian of the global state can be written as

$$H_{int} = \sum_n |n\rangle\langle n| \otimes \widetilde{\Phi}_n \tag{2.2.6}$$

Where the $\widetilde{\Phi}_n$ are arbitrary but dependent on the index n, and act only on the Hilbert space of the measurement system. Evolving an initial state to be measured, the linearity of the Schroedinger equation gives

$$\begin{aligned}\left(\sum_n a_n|n\rangle\right) \ |\Phi_0\rangle \ &\xrightarrow{t} exp(-iH_{int}t)\sum_n a_n|n\rangle \ |\Phi_0\rangle \\ &= \left(\sum_n a_n|n\rangle\right) exp(-i\widetilde{\Phi}_n t)|\Phi_0\rangle \\ &= \sum_n a_n|n\rangle|\Phi_n(t)\rangle\end{aligned} \tag{2.2.7}$$

Which is a correlated state, representing all the possible outcomes of the measurement. Considering the system of interest locally, we write it in tems of the density matrix:

$$\rho_s = \sum_{n,m} a_n a_m^* |n\rangle\langle m||\Phi_m\rangle\langle\Phi_n| \tag{2.2.8}$$

But, assuming that the states of the enviroment are orthonormal $\langle\Phi_m|\Phi_n\rangle = \delta_{mn}$, that is, if the measurement system states discriminate system states the density matrix becomes diagonal in this basis [4]:

$$\rho_s \xrightarrow{t} \sum_n |a_n|^2 |n\rangle\langle n| \tag{2.2.9}$$

The idea above is very limited, since some peculiar considerations were made to get the result above. In fact, this result is achieved only if the Hamiltonian of interaction comutes with the Hamiltonian of the system of interest, and also with the Hamiltonian of the measurement instrument. Nevertheless, this example ilustrates that if we consider the enviroment as being the measurement instrument and that there is an interaction with the system of interest, the quantum effects of the superposition won't be observed in the subsystem of interest. We must also emphasize that the example above is not a solution for the measurement problem, it is just an effect of apparent collapse [4]. It is also possible to show that the decoherence effects can be nulified,

making the subsystem present superpositions again, for example if we isolate the subsystem from the enviroment [29].

To work with the theory of Quantum Open Systems in the following sections, we will use the density matrix formalism, which we will now present in more detail.

2.3 Density Matrix

We are going to use the density operator, which is represented by

$$\rho \equiv \sum_n \lambda_n \left|\psi_n\right\rangle \left\langle\psi_n\right| \tag{2.3.1}$$

Where $\lambda_n \geq 0$ for every n, and $\sum_n \lambda_n = 1$ for normalized states.

From this definition, it can be shown that the density operator has some properties that are always valid [30], which are:

1: The density operator is hermitian:

$$\rho = \rho^\dagger \tag{2.3.2}$$

2: The trace of the density operator is equal to one:

$$\mathrm{Tr}\rho = 1 \tag{2.3.3}$$

3: The density operator is positive semi-definite:
Given a state $|\phi\rangle$, we have:

$$\langle\phi|\rho|\phi\rangle \geq 0 \tag{2.3.4}$$

For all ϕ.

Being positive semi-definite also means that, if α_i are the eigenvalues of ρ, then $\alpha_i \geq 0$ for all i.

This operator will be represented by a hermitian matrix:

$$\rho = \begin{pmatrix} \rho_{11} & \rho_{12} & \cdots & \rho_{1j} \\ \rho_{21} & \rho_{22} & \cdots & \rho_{2j} \\ \cdots & \cdots & \cdots & \cdots \\ \rho_{i1} & \rho_{i2} & \cdots & \rho_{ij} \end{pmatrix} \tag{2.3.5}$$

Where

$$\rho_{ij} = \sum_{i,j} \left|\psi_i\right\rangle \left\langle\psi_j\right| \tag{2.3.6}$$

The expected value of an operator A is given by:

$$\langle A\rangle = \mathrm{Tr}\{\rho A\} \tag{2.3.7}$$

The time evolution of the density operator is defined by the Liouville Equation, which here is in natural units:

$$\frac{d}{dt}\rho(t) = -i[H, \rho(t)] \tag{2.3.8}$$

It's important to point out that the Liouville Equation gives the time evolution of the density operator of the global system, so the Hamiltonian must be that of the global system. In the way we presented it so far, the Liouville Equation works also in usual Quantum Mechanics [1].

2.4 Quantum Open Systems: Subsystem of Interest and Partial Trace

Given that we will study a global system which will be divided in a subsystem of interest and an enviroment, we must create a notation to distinguish them. So, in the development of our study, we will denote the subsystem of interest by S, the enviroment by R, and the Hilbert Space of the global system will be the coupling between the Hilbert Space of the system of interest and the Hilbert Space of the enviroment: $\mathcal{H}_{\mathcal{S}} \otimes \mathcal{H}_{\mathcal{R}}$.

The goal here is to obtain information only from the subsystem of interest.

Our enviroment will be defined as a thermal reservoir at a given temperature, and we define our global initial state as made by noncorrelated states:

$$|\psi\ \rangle = |\phi_S \otimes \phi_R\ \rangle = |\phi_S \phi_R\ \rangle \tag{2.4.1}$$

Writing our global state in terms of the density operator we have:

$$\rho_{S+R} = \rho_S \otimes \rho_R \tag{2.4.2}$$

To obtain information only of our subsystem of interest we will apply an operation called Partial Trace, in which we make a sum over all the enviroment states.

The definition of Partial Trace is:

$$\mathrm{Tr_R}\left[\rho_{S+R}\right] = \mathrm{Tr_R}\left[\rho_S \otimes \rho_R\right] = \rho_S \tag{2.4.3}$$

And the matrix elements of ρ_S, which is obtained from the Partial Trace, are given by:

$$\langle u_n|\rho_S|u'_n\rangle = \sum_p \langle u_n|\langle v_p|)\rho(|u'_n\rangle|v'_p\rangle) \tag{2.4.4}$$

Where $\{|v_p\rangle\}$ is an orthonormal basis of $\mathcal{H}_{\mathcal{R}}$ and $\{|u_n\rangle\}$ is an orthonormal basis of $\mathcal{H}_{\mathcal{S}}$.

Considering that we suppose that the enviroment is in thermal equilibrium at a given reference temperature, that the number of enviroment states is finite and not variable in time, and remembering that the sum over all states is equal to 1 by the normalization condition, we can see that the partial trace must give information only from our subsysem of interest:

To see more clearly the role of the Partial Trace, consider the following example. Let A_S be an operator acting in $\mathcal{H}_{\mathcal{S}}$, and $A_{S+R} = A_S \otimes \mathbb{1}_R$ its extension in $\mathcal{H}_{\mathcal{S}} \otimes \mathcal{H}_{\mathcal{R}}$, where $\mathbb{1}_R$ is the identity operator in $\mathcal{H}_{\mathcal{R}}$.

Using (2.1.4) and the closure relation on the basis $\{|u_n\rangle|v_p\rangle\}$, where $|u_n\rangle$ is a basis of $\mathcal{H}_\mathcal{S}$ and $|v_p\rangle$ is a basis of $\mathcal{H}_\mathcal{R}$, we have:

$$\begin{aligned}\langle A_{S+R}\rangle &= \mathrm{Tr}\{\rho A_{S+R}\} \\ &= \sum_{n,p}\sum_{n',p'}(\langle u_n|\langle v_p|)\rho(|u'_n\rangle|v'_p\rangle) \times (\langle u'_n|\langle v'_p|)A_S \otimes I_R(|u_n\rangle|v_p\rangle) \\ &= \sum_{n,p}\sum_{n',p'}(\langle u_n|\langle v_p|)\rho(|u'_n\rangle|v'_p\rangle) \times \langle u'_n|A_S|u_n\rangle\langle v'_p|v_p\rangle\end{aligned} \tag{2.4.5}$$

But,

$$\langle v'_p|v_p\rangle = \delta_{pp'} \tag{2.4.6}$$

And so:

$$\langle A_{S+R}\rangle = \sum_{n,n'}\left[\sum_p \langle u_n|\langle v_p|)\rho(|u'_n\rangle|v'_p\rangle)\right]\langle u'_n|A_S|u_n\rangle \tag{2.4.7}$$

Inside the brackets we have the matrix element of ρ_S given by the Partial Trace, and therefore:

$$\begin{aligned}\langle A_{S+R}\rangle &= \sum_{n,n'}\langle u_n|\rho_S|u'_n\rangle\langle u'_n|A_S|u_n\rangle \\ &= \sum_n \langle u_n|\rho_S A_S|u_n\rangle \\ &= \mathrm{Tr}\{\rho_S A_S\}\end{aligned} \tag{2.4.8}$$

And so we can see that the partial trace allow us to obtain information of the subsystem of interest as if it were isolated [30].

2.5 Time Evolution in Quantum Open Systems

To use the Liouville Equation to study the time evolution of our system it is important that we use our global system, or in other words, that we include the subsystem of interest and also the enviroment. Hence, we must have:

$$\frac{d}{dt}\rho_{S+R}(t) = -i[H_{tot}, \rho_{S+R}(t)] \tag{2.5.1}$$

And, we represent the operator evolved in time by the following transformation:

$$\rho_{S+R} \to \rho_{S+R}(t) = U\rho_{S+R}(0)U^\dagger \tag{2.5.2}$$

Where $U = e^{-iH_{tot}t}$ when the Hamiltonian, which is the Hamiltonian of the global system, is time-independent.

When we consider the time evolution only of our subsystem of interest, we look for a transformation like the following:

$$\rho_S \to \rho_S(t) \equiv \Lambda\rho_S = Tr_R(U(\rho_S \otimes \rho_R)U^\dagger) \tag{2.5.3}$$

Which is a transformation regarding what we call the reduced dynamics of the subsystem S.

In the equation above we used the Partial Trace to get information of the time evolution of the subsystem of interest only.

As was said before, the Liouville Equantion does not hold for the subsystem S, but it is possible to find an equation for the time evolution of the subsystem.

The derivation of the equation for the reduced dynamics of S won't be done here, but it can be found in the reference [1] where it is assumed that the coupling between the enviroment and the subsystem of interest is weak enough in order to be possible to apply a Markov approximation, which neglects memory effects [4].

In the the case of vacuum neutrino oscillations, which is the case we are going to study, it is reasonable to assume that the coupling between the subsystem and the enviroment is weak since we know that the model of vacuum neutrino oscillations already describes well the experimental data, and so, if there is an effect that arises from the coupling with the enviroment, this effect must be small.

The equation that define the time evolution of the subsystem is known as Lindblad-Kossakowski Equation:

$$\frac{d}{dt}\rho(t) = L\rho = -i[H,\rho] + \frac{1}{2}\sum_{k=1}^{N^2-1}\left([V_k, \rho V_k^\dagger] + [V_k\rho, V_k^\dagger]\right) \tag{2.5.4}$$

Where N is the dimension of the Hilbert space of the subsystem of interest. In this equation we see a Hamiltonian term, which is equal to the one we have on the Liouville Equation, but we also have a non-Hamiltonian term, which appears because we are dealing with an open system, different from what we have in usual Quantum Mechanics, where the system is considered isolated.

The non-Hamiltonian term will be referred here from now on as dissipator.

We will impose on this equation that the entropy increases with time. Using the Von Neumann entropy it is possible to show that this condition leads to restrictions on the operator V_k, in particular we see that it must be hermitian [1].

Supposing that the enviroment have a big number of degrees of freedom, and that it is at a reference temperature, we can suppose that its entropy will not change with time.

Therefore, imposing that the entropy of the global system increases with time, we can consider that only the entropy of the subsystem of interest will increase with time. So we see that the dissipator would evolve a pure state to a state of maximal mixing assintotically.

Given that in this work we will consider the neutrino oscillation in two families, the Lindblad-Kossakowski Equation will be expanded in the basis of $SU(2)$ matrices.

For the Hamiltonian term we have a parametrization which has a form of an antisymmetric matrix:

$$-i[H,\rho(t)] = 2\epsilon_{ijk}H_i\rho_j\sigma_k \tag{2.5.5}$$

And with $V_k = a_\eta^k\sigma_\eta$, we write the non-Hamiltonian term as:

$$D[\rho(t)] = \sum_j\left[2a_m^j a_n^j - \delta_{mn}\sum_k(a_k^j a_k^j)\right]\rho_m\sigma_n = D_{mn}\rho_m\sigma_n \tag{2.5.6}$$

Where the dissipative matrix can have the following parameterization:

$$D_{mn} = -\begin{pmatrix} \frac{1}{2}(\gamma_1 - \gamma_2 - \gamma_3) & \alpha & \beta \\ \alpha & \frac{1}{2}(\gamma_2 - \gamma_1 - \gamma_3) & \delta \\ \beta & \delta & \frac{1}{2}(\gamma_3 - \gamma_2 - \gamma_1) \end{pmatrix} \tag{2.5.7}$$

Here, we parametrized the dissipative matrix in the form of a symmetric matrix. We do so because if we had chosen an arbitrary parametrization, we could have separated it in two matrices, a symmetric and an antisymmetric one, and the antisymetric term could have been added to the Hamiltonian term (since it also has an antisymetric form). Given that the terms which come from the usual Quantum Mechanics have an antisymmetric form, choosing a symmetric parametrization for the dissipative matrix means we are only considering new terms, which couldn't come from usual Quantum Mechanics.

Since $\rho(t)$, is a density operator, all of the properties of a density operator must hold for $\rho(t)$, and since the dissipative matrix D_{mn} is one of the terms of $\rho(t)$, we must impose the properties of a density operator to D_{mn}.

As we said in the first section of this chapter, the density operator has the following properties:

1. The density operator is hermitian.

2. Its trace is equal to one: $\mathrm{Tr}\rho = 1$.

3. The density operator is positive semi-definite. Which means that, given a state $|\phi\rangle$, we have that $\langle\phi|\rho|\phi\rangle \geq 0$ for all ϕ.

Therefore, the matrix D_{mn} must also be hermitian and positive semi-definite. Hence, it must obey the following inequalties [1]:

$$RST \geq 2\alpha\beta\delta + R\alpha^2 + S\beta^2 + T\delta^2 \tag{2.5.8}$$

Where

$$\begin{array}{lll} 2R \equiv \gamma_1 + \gamma_2 - \gamma_3 \geq 0 & ; & RS - \alpha^2 \geq 0 \\ 2S \equiv \gamma_1 + \gamma_3 - \gamma_2 \geq 0 & ; & RT - \beta^2 \geq 0 \\ 2T \equiv \gamma_2 + \gamma_3 - \gamma_1 \geq 0 & ; & ST - \delta^2 \geq 0 \end{array} \tag{2.5.9}$$

With the conditions above, the dissipative matrix Eq. (2.5.7) will be hermitian and positive semi-definite except for the minus sign that comes from the comutation relations in the non-Hamiltonian term.

We still need to verify the necessary conditions for $\mathrm{Tr}\rho(t) = 1$. This condition is related to the normalization of the sum of the probabilities of all the posssible states.

If we want the number of states to remain equal during the entire time evolution, we must impose the conservation of the probability, which is done by imposing $\mathrm{Tr}[\dot{\rho}(t)] = 0$. Applying this condition to both sides of the Lindblad-Kossakowski Equation, we have, for the left side:

$$\frac{d}{dt}\mathrm{Tr}\rho(t) = \mathrm{Tr}[\dot{\rho_\mu}\sigma_\mu] = 0 \;\; \Rightarrow \;\; \dot{\rho_0} = 0 \tag{2.5.10}$$

So, we see that we must always have $\rho_0(t) = \rho_0(0)$.

And for the right side:

$$\mathrm{Tr}[\dot{\rho}(t)] = \mathrm{Tr}[2\epsilon_{ijk}H_i\rho_j\sigma_k + \rho_\nu D_{\mu\nu}\sigma_\mu] \tag{2.5.11}$$

Since $\mathrm{Tr}[\sigma_0] = 2$, from the equation above, we have:

$$2\rho_\nu D_{0\nu} = 0 \quad \Rightarrow \quad D_{0\nu} = 0 \tag{2.5.12}$$

Because ρ_ν is arbitrary, real, and positive.

The complete form of the Lidblad-Kossakowski Equation expanded in the basis of SU(2) matrices is the following

$$\frac{d}{dt}\rho_\mu(t)\sigma_\mu = 2\epsilon_{ijk}H_i\rho_j(t)\sigma_\mu\delta_{\mu k} + D_{\mu\nu}\rho_\nu\sigma_\nu \tag{2.5.13}$$

With $D_{\mu 0} = D_{0\nu} = 0$, where $D_{0\nu} = 0$ comes from the condition of conservation of probaility, and $D_{\mu 0} = 0$ because we chose a symmetric parametrization for the dissipator.

This equation will be used to obtain new neutrino oscillation probabilities, considering different forms of the dissipator which obey the conditions above.

Since it was derived considering the inclusion of the enviroment, different from what is done in usual Quantum Mechanics, we will find oscilation probabilities which are different from the one we know for the case of oscillation in two families. The goal is to use the new probabilities in a study with experimental data, and verify their validity. Later in this work we will show the results of this study considering data from the KamLAND experiment.

References [1,15,32-34] present very good studies about quantum dissipation and decoherence, such as other analysis using data from other experiments.

Chapter 3

Neutrino Oscillations

Since the experimental verification of the neutrino oscillation phenomenon, several works have been made, and we can see that the models that describe them lead to the conclusion that the neutrinos have mass, different from what was estabilished in the minimal version of the Standard Model.

The description of the neutrino oscillation is based on the superposition principle, which is a fundamental feature of Quantum Mechanics, and from this description we can see that the oscillations would go on indefinitely.

Given that the usual approach used to study neutrino oscillations is based entirely on usual Quantum Mechanics, this is an approach that does not include a coupling with the enviroment. Our goal here is to change that.

As was said before, we will use the equations derived in the previous chapter to study the effect of the coupling with the enviroment, and we will see that in this model the superpositions will not be the same as in the usual approach, and that will lead to different equations for the oscillation probabilities.

But first we will study neutrino oscillation in the case where there is no coupling with the enviroment. Here we will consider only vacuum neutrino oscillations, and we will use the density matrix formalism.

This study will be made here in more detail, since it presents the method that will be used to find all the different oscillation probabilities.

3.1 3.1 Vacuum Neutrino Oscillation: Density Matrix

Currently, there is experimental verification of the existence of three neutrino families, and so there are three flavour eigenstates and three mass eigenstates.

In this work though, we will consider for simplicity only neutrino oscillation in two families.

The relation between mass eigenstates and flavour eigenstates is given by

$$\begin{pmatrix} \nu_\alpha \\ \nu_\beta \end{pmatrix} = U \begin{pmatrix} \nu_1 \\ \nu_2 \end{pmatrix} \tag{3.1.1}$$

Where the $\nu_{(\alpha,\beta)}$ are the flavour eigenstates, and the $\nu_{(1,2)}$ are the mass eigenstates.

The matrix U is a rotation matrix, known in this case as mixing matrix.

In the formalism for two families we use the rotation matrix in $SU(2)$, which is

$$U = \begin{pmatrix} \cos\theta & \sin\theta \\ -\sin\theta & \cos\theta \end{pmatrix} \tag{3.1.2}$$

Where θ is the mixing angle.

If we were to study neutrino oscillations in three families, we would only need to include a third neutrino flavour eigenstate and a third neutrino mass eigenstate, and substitute the rotation matrix in $SU(2)$ for the rotation matrix in $SU(3)$.

As was said before, we are going to use the density matrix formalism.

In the previous chapter we found the time evolution equation, called Lindblad-Kossakowski Equation, which expanded in the basis of $SU(2)$ matrices is:

$$\frac{d}{dt}\rho_\mu(t)\sigma_\mu = 2\epsilon_{ijk}H_i\rho_j(t)\sigma_\mu\delta_{\mu k} + D_{\mu\nu}\rho_\nu\sigma_\mu \tag{3.1.3}$$

But now, we are going to consider that there is no coupling with the enviroment, an so the non-Hamiltonian term vanishes:

$$D_{\mu\nu} = 0 \tag{3.1.4}$$

Therefore, we have simply the Liouville Equation:

$$\frac{d}{dt}\rho_\mu(t)\sigma_\mu = 2\epsilon_{ijk}H_i\rho_j(t)\sigma_\mu\delta_{\mu k} \tag{3.1.5}$$

Using the approximation:

$$E_i = \sqrt{\mathbf{p}^2 + m_i^2} \simeq |\mathbf{p}| + \frac{m_i^2}{2|\mathbf{p}|} \tag{3.1.6}$$

which is valid when $m_i \ll |\mathbf{p}|$, we can write the Hamiltonian of the system as:

$$H = \begin{pmatrix} E + \frac{m_1^2}{2E} & 0 \\ 0 & E + \frac{m_2^2}{2E} \end{pmatrix} \tag{3.1.7}$$

Now, we must expand it in the basis of $SU(2)$ matrices and solve the Liouville Equation. We then find:

$$\begin{aligned} &\rho_0(t) = \rho_0(0); \\ &\rho_1(t) = \rho_1(0)\cos(\tfrac{\Delta m^2}{2E}t); \\ &\rho_2(t) = -\rho_1(0)\sin(\tfrac{\Delta m^2}{2E}t); \\ &\rho_3(t) = \rho_3(0); \end{aligned} \tag{3.1.8}$$

We make the assumption that the source creates neutrinos of a single flavour. So, the density matrix of the initial state is given by:

$$\rho(0) = |\nu_\alpha\rangle\langle\nu_\alpha| \tag{3.1.9}$$

But, in the mass eigenstate basis we have:

$$|\nu_\alpha\rangle = \cos\theta|\nu_1\rangle + \sin\theta|\nu_2\rangle \tag{3.1.10}$$

So that:

$$\rho(0) = \begin{pmatrix} \cos^2\theta & \frac{1}{2}\sin(2\theta) \\ \frac{1}{2}\sin(2\theta) & \sin^2\theta \end{pmatrix} \tag{3.1.11}$$

This initial state will be expanded in the basis of $SU(2)$ matrices and substituted in the solution found before (3.1.8). Therefore the solution is:

$$\begin{array}{l} \rho_0(t) = \frac{1}{2}; \\ \rho_1(t) = \frac{1}{2}\sin(2\theta)\cos(\frac{\Delta m^2}{2E}t); \\ \rho_2(t) = -\frac{1}{2}\sin(2\theta)\sin(\frac{\Delta m^2}{2E}t); \\ \rho_3(t) = \frac{1}{2}\cos(2\theta); \end{array} \tag{3.1.12}$$

Which in the matrix form is:

$$\rho(t) = \begin{pmatrix} \rho_0(t) + \rho_3(t) & \rho_1(t) - i\rho_2(t) \\ \rho_1(t) + i\rho_2(t) & \rho_0(t) - \rho_3(t) \end{pmatrix} = \begin{pmatrix} \frac{1}{2} + \frac{1}{2}\cos(2\theta) & \frac{1}{2}e^{i(\frac{\Delta m^2}{2E}t)} \\ \frac{1}{2}e^{-i(\frac{\Delta m^2}{2E}t)} & \frac{1}{2} - \frac{1}{2}\cos(2\theta) \end{pmatrix} \tag{3.1.13}$$

We will assume that the neutrinos are relativistic, and then we will change the spatial parameter for a time parameter.

So, the final form of the evolved density matrix is:

$$\rho(x) = \begin{pmatrix} \frac{1}{2} + \frac{1}{2}\cos(2\theta) & \frac{1}{2}e^{i(\Delta x)}\sin(2\theta) \\ \frac{1}{2}e^{-i(\Delta x)}\sin(2\theta) & \frac{1}{2} - \frac{1}{2}\cos(2\theta) \end{pmatrix} \tag{3.1.14}$$

Where $\Delta = \frac{\Delta m^2}{2E}$.

In this density matrix, the elements of the main diagonal are known as population terms. They give the probabilities of survival and transition, repectively. To see the usual form of these probabilities we would still need to change them to the basis of flavor eigenstates.

The terms which are out of the main diagonal are known as coherence terms, and they determine the oscillatory behaviour of the probabilities.

To obtain the equation for the probability oscillation we use that:

$$P_{\nu_\alpha \to \nu_\alpha} = Tr[\rho(0)\rho(t)] = 2\rho_\mu(0)\rho_\mu(t) \tag{3.1.15}$$

And then we get:

$$P_{\nu_\alpha \to \nu_\alpha}(x, E) = 1 - \sin^2(2\theta)\sin^2(\frac{\Delta}{2}x) \tag{3.1.16}$$

Which is the usual equation for the survival probability in vacuum neutrino oscillations in two families.

3.2 3.2 Neutrino Oscillation and Quantum Open Systems: Case 1

Now that we know how to use the density matrix formalism to get the probabilities for vacuum neutrino oscillations, it is time to do a more complete work, considering now the coupling with the enviroment.

We will do that by considering possible forms of the non-Hamiltonian term in the Lindblad-Kossakowski Equation, and by solving it we will find different forms for the oscillation probabilities.

In the first case considered, we will impose that

$$[V_k, H_{osc}] = 0 \tag{3.2.1}$$

Where H_{osc} is the Hamiltonian of the oscillations, so it is the Hamiltonian of the subsystem of interest, and the operator V_k acts in the interaction between the subsystem S and the enviroment, by bringing to S the perturbations from the enviroment.

This assumption is equivalent as assuming that the subsystem of neutrinos has it's energy average value conserved.

It can be shown that the consequence of this assumption is that we have a dissipative matrix with only one phenomenological parameter [1], which we will call γ, and the matrix is given by:

$$D_{\mu\nu} = diag\{0, -\gamma, -\gamma, 0\} \tag{3.2.2}$$

We now must use this form of the dissipator in the Lindblad-Kossakowski Equation, expand it in the bais of $SU(2)$ matrices and solve it, similar to what was done in the previous section for the vacuum neutrino oscillations, except that now the dissipator has the form above.

We then get for the evolved density matrix:

$$\rho(x) = \begin{pmatrix} \frac{1}{2} + \frac{1}{2}\cos(2\theta) & \frac{1}{2}e^{-(\gamma - i\Delta)x}\sin(2\theta) \\ \frac{1}{2}e^{-(\gamma + i\Delta)x}\sin(2\theta) & \frac{1}{2} - \frac{1}{2}\cos(2\theta) \end{pmatrix} \tag{3.2.3}$$

Here we can see that in the coherence terms, which are the ones out of the main diagonal, there is a term of exponential decay which depends on γ.

Hence, we see that there is an elimination of the quantum coherence throughout the propagation of the neutrino.

Therefore, from this form of the dissipation matrix arises an effect of quantum decoherence.

Using equations (3.1.14) and (3.1.15) we can obtain the oscillation probability case 1:

$$P^{C_1}_{\nu_\alpha \to \nu_\alpha}(x, E) = 1 - \sin^2(2\theta)[1 - e^{-\gamma x}\cos(\Delta x)] \tag{3.2.4}$$

Where again we see the exponential of $-\gamma$, which acts as a dumping.

3.3 3.3 Neutrino Oscillation and Quantum Open Systems: Case 2

Now we will consider a different form of the dissipative matrix, in which we will include another parameter in the last entry of the main diagonal.

Remembering that it must follow the conditions estabilished by inequalties (2.5.8) and (2.5.9), we see that this new parameter can be at most equal to the sum of elements D_{11} and D_{22}.

Since maximizing this parameter will not help us from a phenomenological point of view, we will simply assume that it is equal to the parameter of the previous case. Hence, the dissipative matrix will have the following form:

$$D_{\mu\nu} = diag\{0, -\gamma, -\gamma, -\gamma\} \tag{3.3.1}$$

Again we will substitute it in the Lindblad-Kossakowski Equation, expand it in the basis of $SU(2)$ matrices and solve it. Then, we will find the following evolved density matrix:

$$\rho(x) = \begin{pmatrix} \frac{1}{2} + \frac{1}{2}e^{-\gamma x}\cos(2\theta) & \frac{1}{2}e^{-(\gamma - i\Delta)x}\sin(2\theta) \\ \frac{1}{2}e^{-(\gamma + i\Delta)x}\sin(2\theta) & \frac{1}{2} - e^{-\gamma x}\frac{1}{2}\cos(2\theta) \end{pmatrix} \tag{3.3.2}$$

In this case we also see the dumping term on the coherence terms, which eliminates the coherence throughout the propagation, but now we also have a new effect.

We can see that the population terms also have a dumping exponential, which leads to an assintotic limit of $\frac{1}{2}$, which means that we have flavour convertion.

Even when we eliminate the quantum superposition, by making $\theta = 0$, we would still have an assintotic limit of $\frac{1}{2}$ for the population terms.

Therefore, the simple adition of a parameter on D_{33} leads to an effect of flavour convertion apart from quantum superpositions, apart from oscillations.

From equations (3.3.2) and (3.1.15) we get the oscillation probability for this case 2:

$$P^{C_2}_{\nu_\alpha \to \nu_\alpha}(x, E) = \frac{1}{2} + e^{-\gamma x}\left[\frac{1}{2} - \sin^2(2\theta)\sin^2(\frac{\Delta}{2}x)\right] \tag{3.3.3}$$

Where we can also see the assintotic limit of $\frac{1}{2}$ for the survival probability, even when there is no quantum superposition [15].

Chapter 4

KamLAND and Simulation

Since we want to confront the results we obtained on the previous chapters with experimental data, it is important that we examine the fundamental features of neutrino experiments and of the methods of verification of the validity of a scientific model.

Therefore, in this chapter we will first present a short review of neutrino experiments, and mainly the KamLAND experiment, which data we will use on the next chapter of this work.

Then, we will present the χ^2 Test used for the analysis, and the details of the program used for the simulations.

4.1 Neutrino Experiments and KamLAND

The characterization of a neutrino oscillation experiment is defined by the typical energy E of the neutrino, and by the distance L between the source and the detector. But, we know that in general, the neutrino beams analyzed by the experiments are not monoenergetic, and also that the detectors' energy resolution is finite. So, instead of measuring a probability $P_{\alpha\beta}$ of transition between a state α and a state β, the experiments are sensitive to the average probability [6]:

$$\langle P_{\alpha\beta} \rangle = \frac{\int dE \frac{d\Phi}{dE} \sigma_{CC}(E) P_{\alpha\beta}(E) \epsilon(E)}{\int dE \frac{d\Phi}{dE} \sigma_{CC}(E) \epsilon(E)} \tag{4.1.1}$$

Where Φ is the neutrino energy spectrum, σ_{CC} is the cross section for the process in which the neutrino is detected (which is in general, a Charged Current interaction), $\epsilon(E)$ is the detection efficiency, and the range of the energy integral depends on the energy resolution of the experiment.

Typical values of L/E for diferent kinds of experiments and neutrino sources, and the correspondent orders of magnitude of Δm^2 to which they are most sensitive can be seen in Table 4.1.

Since we have that [6]

$$L_{0,ij}^{osc} = \frac{4\pi E}{\Delta m_{ij}^2} \tag{4.1.2}$$

Experiment	L(m)	E(MeV)	$\Delta m^2(\text{eV}^2)$
Solar	10^{10}	1	10^{-10}
Atmospheric	$10^4 - 10^7$	$10^2 - 10^5$	$10^{-1} - 10^{-4}$
Reactor	$10^2 - 10^3$ $10^4 - 10^5$	1	$10^{-2} - 10^{-3}$ $10^{-4} - 10^{-5}$
Accelerator	10^2 $10^5 - 10^6$	$10^3 - 10^4$ 10^4	> 0.1 $10^{-2} - 10^{-3}$

Table 4.1: Characteristic values of L and E for various neutrino sources and experiments and the corresponding ranges of Δm^2 to which they can be most sensitive.

If we want the experiment to be sensitive to a given value of Δm^2_{ij}, it must be set up with $(L/E) \approx \Delta m^2_{ij}(L^{osc}_{0,ij} \sim L)$, otherwise, if $(L/E) \gg \Delta m^2_{ij}(L^{osc}_{0,ij} \gg L)$ the oscillation phase doesn't have enough time to have an appreciable effect, and if $(L/E) \ll \Delta m^2_{ij}(L^{osc}_{0,ij} \ll L)$ the oscillation phase goes through many cycles before the detection,and we will see an average $\left\langle \sin^2\left(\frac{\Delta m^2_{ij} L}{4E}\right)\right\rangle = \frac{1}{2}$.

To maximize sensitivity, the following conditions should be fulfilled [6]:

- $E/L \approx \Delta m^2_{ij}$
- Good energy resolution for the experiment, $\Delta E \ll L\Delta m^2_{ij}$
- Experiment is sensitive to different values of L with $\Delta L \ll E/\Delta m^2_{ij}$

4.1.1 KamLAND

In this work, we are going to use data from the KamLAND experiment.

KamLAND is a Long Baseline experiment, located at the Kamioka mine, Gifu, Japan, made to detect electron antineutrinos which come from nuclear reactors being at an average distance of $\sim$ 180km from the detector. Figure (4.1) shows the location of KamLAND and the main nuclear power stations in Japan.

The main target consists of 1kt of liquid scintilator, and this internal detector is shielded by an external detector of Cherenkov light in water of 3.2kt. A more detailed review of the experiment can be found in reference [8].

The detection of the $\bar{\nu}_e$ is done by the inverse β decay:

$$\bar{\nu}_e + p \to e^+ + n \tag{4.1.3}$$

Since the electron antineutrinos travel through the terrestrial crust between the reactors and the detector, matter effects are usually considered when dealing with KamLAND data, and a constant density of $2.7 g/cm^3$ is considered for the terrestrial crust.

The KamLAND experiment was constructed to test the so called Large Mixing Angle (LMA) solution for the solar neutrino problem, which consisted of a solar neutrino detection rate which

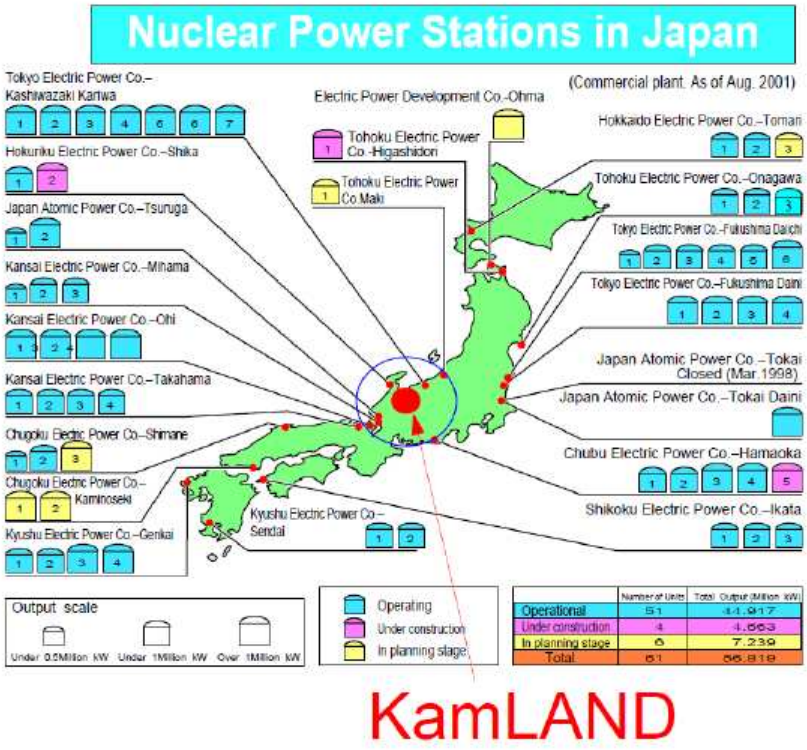

Figure 4.1: Location of KamLAND and main power stations in Japa. The blue circle indicates the average distance of 180km. [7]

was substantially smaller than that predicted by standard solar models. Typical values of the parameters for the LMA solution are [5]:

$$\Delta m^2 \sim 7 \times 10^{-5} eV^2 \quad \tan^2(\theta) \sim 0.4$$

Considering the average value of L, and that the energy of the electron antineutrinos is on the order of MeV, it is sensitive to $\Delta m^2_{ij} \gtrsim 10^{-5} eV^2$ [6].

We see then, that we have an important relation between solar neutrino experiments and KamLAND, in which KamLAND provides precision in the measurement of Δm^2, and solar neutrinos provide precision in the measurement of $\tan^2(\theta)$ due to particularities of the two kinds of experiments [5], allowing a more precise study of the solar parameters.

4.2 The χ^2 Test

Before we present the results of the tests, it's important to define the model used for the χ^2 Test:

$$\chi^2 \equiv \sum_j^n 2\left[KN_j^{theo} - N_j^{obs} + N_j^{obs} ln\left(\frac{N_j^{obs}}{KN_j^{theo}}\right)\right] \tag{4.2.1}$$

Since the experiment consists of counting events in energy bins, and hence the data are a set of discrete events in continuums intervals, the appropriate model is given by the Poisson statistics [13,31].

In the equation above the sum is made over the n energy bins (energy intervals), N_j^{theo} is the number of events expected in accordance to the theory, N_j^{obs} is the number of events observed given by the KamLAND Collaboration, both related to a bin j, and K is a free parameter of the model, which represents the flux, and here runs from 0.75 and 1.25.

4.3 Simulation

In this work we used a program originally made by Professor Pedro Cunha de Holanda Ph.D, which makes a χ^2 test and returns the best-fit values of the parameters involved. It also allow us to get confidence level curves for the parameter space considered.

The original program uses data from the KamLAND energy spectrum, and does the chi-square test considering the usual neutrino oscillation probability for the case of two families. It returns the minimum value of chi-square and it's respective Δm^2 and $\tan^2\theta$ values, which are the best-fit values.

We wanted to use this program to verify the limits on γ for the probability with decoherence Case 1, and in order to do that we would need to modify the original program, including a third parameter, which is γ, and changing the expression for the usual neutrino oscillation probability for the first we obtained in the previous chapter.

But before studying the probability with decoherence Case 1, we tested the original program using the usual oscillation probability, to see if it gave a good reproduction for the results of KamLAND.

The data used in this version of the program consider 24 energy bins, and are from the presentation [10] "KamLAND (Anti-Neutrino Status)" from Itaru Shimizu (Tohoku University) on the conference "The 10th International Conference on Topics in Astroparticle and Underground Physics" on 14^{th} September, 2007.

The simulation consists in the calculation of the number of expected events for a given energy interval a (the energy interval is also know as *bin*):

$$N_a = \sum_i^n \int_{E_a}^{E_a+\Delta E} dE_p \int dE_\nu \int dE'_p P_i C_i F_i \sigma f(E_p, E'_p) \tag{4.3.1}$$

Where the sum is over each reactor i, with percentual contribution C_i, P_i is the oscillation probability, which will be the usual one for the test, and the probability Case 1 for the final analysis, F_i is the flux of the reactor, σ is the cross section of the antineutrino detection, $f(E_p, E'_p)$ is the function of energy resolution, and we have integrations over the neutrino energy E_ν, and over the real energy of the positron produced E'_p [6].

Then, we used the χ^2 Test defined on the previous section to get best-fit results and confidence level curves, which we used to obtain the limits for the three parameters in different confidence levels.

We repeated the proceedure described above using a different set of data, which was obtained in the article "Constraints on θ_{13} from a three-flavor oscillation analysis of reactor antineutrinos at KamLAND" (The KamLAND Collaboration) [11] from March 2011.

Chapter 5

Results

After having studied the density matrix formalism, applying it to Quantum Open Systems and using the results obtained to get new neutrino oscillation probabilities, we are ready to make a confrontation with experimental data.

We first present the results for a test of the original program, to verify if it was a good tool to analyse our model.

In the following sessions we will present the results of the tests we made, and also the final results, which are the limits for the parameters involved in neutrino oscillation with decoherence.

5.1 Results for the Usual Case

The program varies Δm^2 and $\tan^2(\theta)$ in the intervals:

$$\begin{array}{ccccc} 0.2 & \leq & \tan^2(\theta) & \leq & 5.0 \\ 6.0 \times 10^{-5} eV^2 & \leq & \Delta m^2 & \leq & 10^{-4} eV^2 \end{array} \tag{5.1.1}$$

The results for the best-fit are given in Table (5.1).

$\chi^2 min = 39.45$
$\Delta m^2 = 7.80^{+0.22}_{-0.20} \times 10^{-5} eV^2$
$\tan^2(\theta) = 0.51^{+0.21}_{-0.10}$

Table 5.1: Best-Fit Results: Original Program

Where the deviations considered in Table (5.1) correspond to 68.27%C.L..

Since we have 24 energy bins, we see on Table (5.1) that the value of χ^2 minimum is of the same order of the number of experimental points, which indicates a good agreement between the theoretical model and the experimental data.

It is important to point out that the program presents another χ^2 minimum, which has an identical value to the one we showed before, it also has the same correspondent value of Δm^2, but for the mixture angle we have the value of $\tan^2 \theta_2 = 1.94$, where $\theta_1 + \theta_2 = 90°$.

$\Delta m^2 = 7.58^{+0.14}_{-0.13}(stat)^{+0.15}_{-0.15}(syst) \times 10^{-5} eV^2$
$\tan^2(\theta) = 0.56^{+0.10}_{-0.07}(stat)^{+0.10}_{-0.06}(syst)$

Table 5.2: Best-Fit Results for KamLAND as presented in reference [9]

The best-fit obtained by the KamLAND Collaboration in reference [9] can be seen in Table (5.2).

In Figure (5.1) we see the confidence level curves for this set of results.

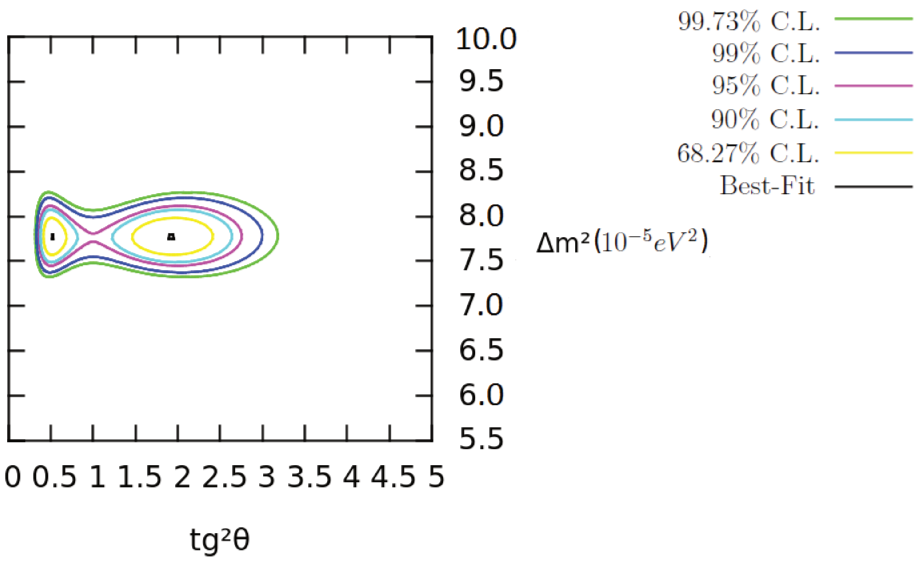

Figure 5.1: Confidence Level Curves for $\tan^2(\theta)$ and Δm^2 made with data from the simulation of the usual model of neutrino oscillation, considering the data from reference [ref]. The curves correspond to 68.27%, 90%, 95%, 99% and 99.73% C.L.

To compare our results with original results from KamLAND we show in Figure (5.2) a graph found in reference [9] where we can see the confidence level curves as presented by the KamLAND Collaboration.

5.2 χ^2 Test: Results For Case 1

After having tested the original program used for the χ^2 test we are ready for the first modifications, in order to analyse the neutrino oscillation probabilities found in the previous chapter.

For the Case 1 we substituted the usual neutrino oscillation probability:

$$P_{\nu_\alpha \to \nu_\alpha}(x, E) = 1 - \sin^2(2\theta)\sin^2(\frac{\Delta}{2}x) \tag{5.2.1}$$

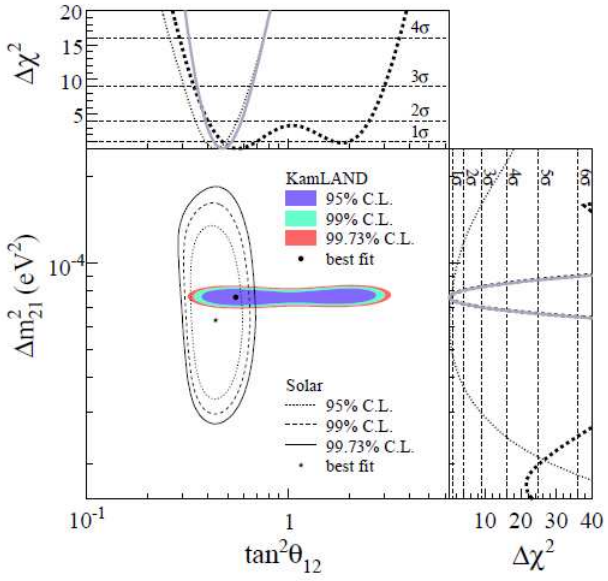

Figure 5.2: Confidence Level Curves for $\tan^2(\theta)$ and Δm^2 as presented by the KamLAND Collaboration in reference [9]

for the probability with decoherence Case 1:

$$P^{C_1}_{\nu_\alpha \to \nu_\alpha}(x, E) = 1 - \sin^2(2\theta)[1 - e^{-\gamma x}\cos(\Delta x)] \tag{5.2.2}$$

and changed the program including a third free parameter, which is the parameter γ. Now, our program varies the three parameters: Δm^2, $\tan^2(\theta)$ and γ.

The three parameters were variated in the intervals:

$$\begin{array}{ccccc} 0.2 & \leq & \tan^2(\theta) & \leq & 3.8 \\ 7.25 \times 10^{-5} eV^2 & \leq & \Delta m^2 & \leq & 8.40 \times 10^{-5} eV^2 \\ 0 & \leq & \gamma & \leq & 7.85 \times 10^{-3} (km)^{-1} \end{array} \tag{5.2.3}$$

In this case, the results for the best fit are given in Table (5.3).

$\chi^2 min = 38.78$
$\Delta m^2 = 7.79 \times 10^{-5} eV^2$
$\tan^2(\theta) = 0.56$
$\gamma = 6.88 \times 10^{-4} km^{-1} = 1.36 \times 10^{-22} GeV$

Table 5.3: Best-Fit Results: Case 1

We can see on Table (5.3) that for the best-fit we have a nonzero value of γ, and it's respective minimum χ^2 value is smaller than the one found for the usual probability without decoherence.

Considering the value of γ obtained here, and considering an average distance from the KamLAND detector to the reactors around it, we can find an average value for the term $e^{-\gamma x}$ of the probability Case 1 which would be:

$$e^{-\gamma x} \sim 0,9 \tag{5.2.4}$$

Which indicates that the KamLAND experiment must have enough sensitivity to observe an effect of this order.

We also made three graphs for the confidence level curves. The Figure (5.3) shows the curves for $\tan^2(\theta)$ versus Δm^2, the Figure (5.4) shows the curves for $\tan^2(\theta)$ versus γ, and the Figure (5.5) shows the curves for Δm^2 versus γ.

All the graphs of the confidence level curves were made considering the data from reference [10], and the curves were chosen in accordance to the PDG Booklet [13] and correspond to confidence levels of 68.27%, 90%, 95%, 99%, 99.73% C.L

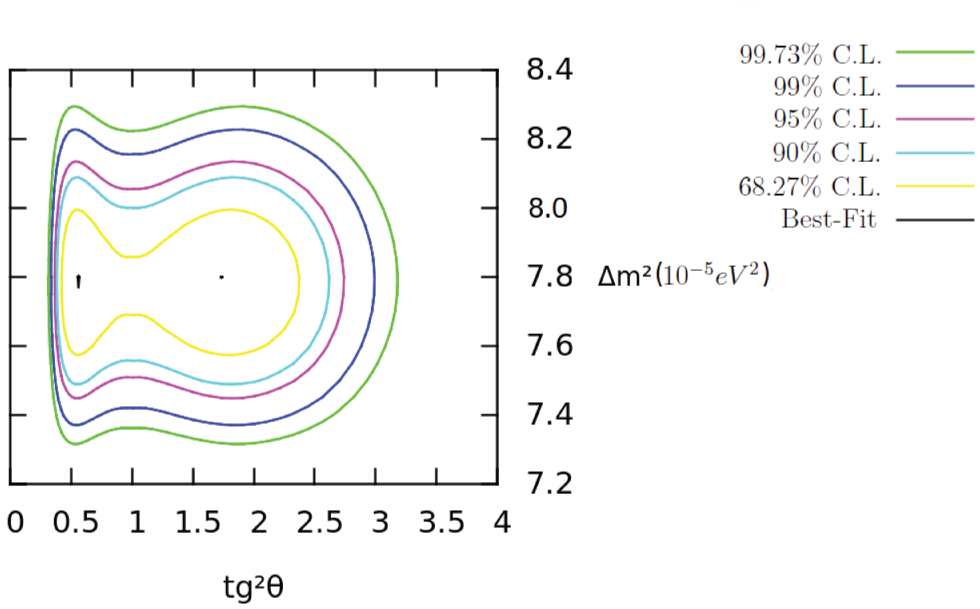

Figure 5.3: Confidence Level Curves for $\tan^2(\theta)$ and Δm^2 made with data from the simulation of our model of oscillation with decoherence considering the data from reference [10]. The curves correspond to 68.27%, 90%, 95%, 99% and 99.73% C.L.

To make the the graphs (Figure (5.3), Figure (5.4), and Figure (5.5)), we proceeded in the following manner: for each graph we made a data table where the values of two paramaters were held fixed, and then χ^2 was minimized in relation to the third parameter [12].

Then, we could use these tables to make a contour plot at $\chi^2_{min} + \Delta\chi^2$ where the values of $\Delta\chi^2$ were chosen in accordance to reference [13] to obtain the confidence level curves.

With the graphs of the confidence level curves we were able to obtain the limits for the three parameters involved, which are given in the table (5.4).

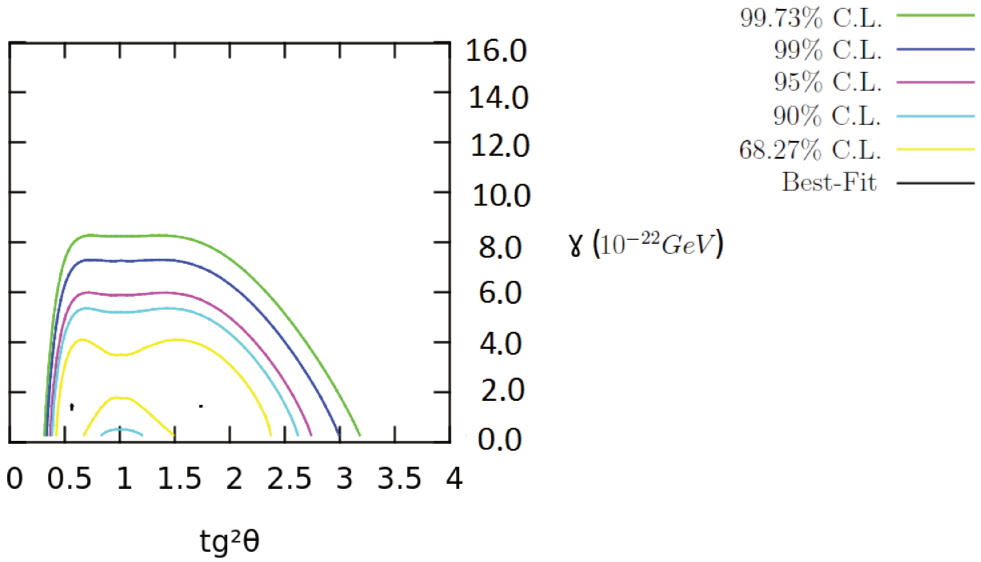

Figure 5.4: Confidence Level Curves for $\tan^2(\theta)$ and γ made with data from the simulation of our model of oscillation with decoherence considering the old data from reference [10]. The curves correspond to 68.27%, 90%, 95%, 99% and 99.73% C.L.

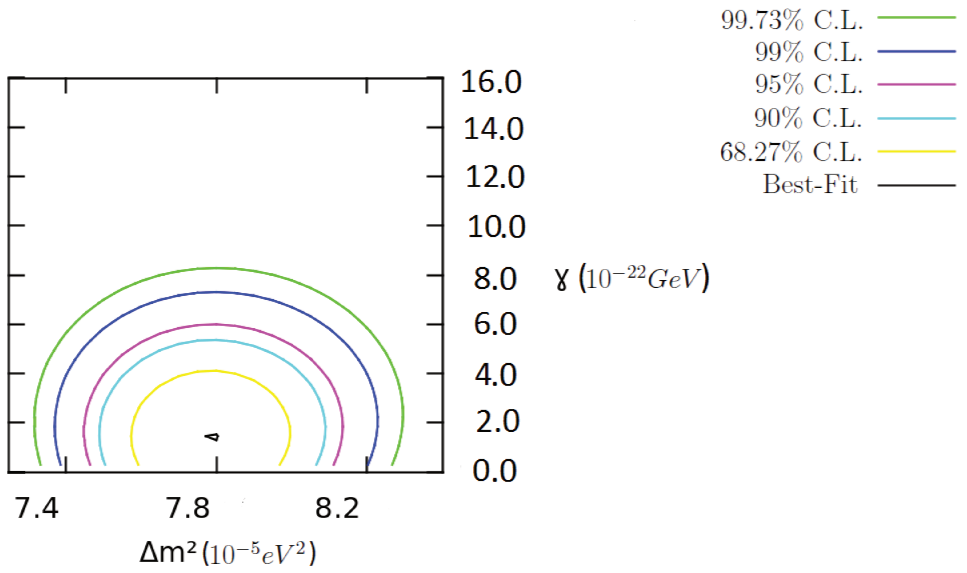

Figure 5.5: Confidence Level Curves for Δm^2 and γ made with data from the simulation of our model of oscillation with decoherence considering the old data from reference [10]. The curves correspond to 68.27%, 90%, 95%, 99% and 99.73% C.L.

68.27% C.L.	$(7.57 < \Delta m^2 < 8,00)10^{-5}eV^2$	$0.42 < \tan^2(\theta) < 2.38$	$(0 < \gamma < 4.13)10^{-22}GeV$
90% C.L.	$(7.49 < \Delta m^2 < 8,09)10^{-5}eV^2$	$0.39 < \tan^2(\theta) < 2.63$	$(0 < \gamma < 5.38)10^{-22}GeV$
95% C.L.	$(7.44 < \Delta m^2 < 8,14)10^{-5}eV^2$	$0.35 < \tan^2(\theta) < 2.74$	$(0 < \gamma < 6.04)10^{-22}GeV$
99% C.L.	$(7.37 < \Delta m^2 < 8,23)10^{-5}eV^2$	$0.33 < \tan^2(\theta) < 3.00$	$(0 < \gamma < 7.33)10^{-22}GeV$
99.73% C.L.	$(7.32 < \Delta m^2 < 8,30)10^{-5}eV^2$	$0.30 < \tan^2(\theta) < 3.18$	$(0 < \gamma < 8.26)10^{-22}GeV$

Table 5.4: Parameter's Limits for Oscillation with Decoherence Case 1

This case was already analysed on the literature by Lisi et al [14], in which was made a combination of solar and KamLAND data. From this analysis it was obtained a best-fit for γ equal to zero, which means that, in their joint analysis of solar and KamLAND data, including decoherence on the neutrino oscillations doesn't improve the fit of the data.

5.3 Most Recent Data χ^2 test: Case 1

The results presented so far do not consider the most recent data.

They were the first results used in our studies, but we also have the results for new data.

In the article "Constraints on θ_{13} from a three-flavor oscillation analysis of reactor antineutrinos at KamLAND" (The KamLAND Collaboration) [11] from March 2011, we have a new set of data, in which they changed the number of energy bins to 20.

For this set of data, we also made a test using the usual oscillation probability, and the comparison between the results for the new and the old data can be seen in the Table (5.5).

	Old data (24 bins)	New Data (20 bins)
χ^2_{min}	39.45	24.88
Δm^2	$7.80 \times 10^{-5}eV^2$	$8.05 \times 10^{-5}eV^2$
$\tan^2(\theta)$	0.51	0.44

Table 5.5: Best-Fit Results Comparison Between New and Old Data for $\gamma = 0$

We can see that not only the value of χ^2_{min} is smaller for the new data, but it is also closer to the number of degrees of freedom, indicating a better agreement with the experimental data.

Considering now the oscillation probability with decoherence Case 1, and the three free parameters Δm^2, $\tan^2(\theta)$ and γ, we can also compare the results for the new and the old data.

The three parameters were variated in the intervals:

$$\begin{array}{ccccc} 0.2 & \leq & \tan^2(\theta) & \leq & 3.8 \\ 7.50 \times 10^{-5}eV^2 & \leq & \Delta m^2 & \leq & 8.65 \times 10^{-5}eV^2 \\ 0 & \leq & \gamma & \leq & 7.85 \times 10^{-3}(km)^{-1} \end{array} \tag{5.3.1}$$

The comparison between the best-fit results for this case can be seen in the Table (5.6).

Where again we see that the value of χ^2_{min} is closer to the number of degrees of freedom for the new data, and therefore we have a better fit.

	Old data (24 bins)	New Data (20 bins)
χ^2_{min}	38.78	21.36
Δm^2	$7.80 \times 10^{-5} eV^2$	$8.05 \times 10^{-5} eV^2$
$\tan^2(\theta)$	0.56	0.54
γ	$6.72 \times 10^{-4} km^{-1} = 1.32 \times 10{-}22 GeV$	$1.6 \times 10^{-3} km^{-1} = 3.15 \times 10^{-22} GeV$

Table 5.6: Best-Fit Results Comparison Between New and Old Data For Three Free Parameters

We can also see that including the third parameter γ improves the fit in both cases (with new and old data), but the decrease in the value of χ^2_{min} for the program with three free parameters is more significant (3.52 unit decrease) than the decrease we see for the program in which we made $\gamma = 0$.

Here we also made confidence level curves, using the same process we used for the old data, and in accordance to the PDG Booklet [13] we chose the values of $\Delta\chi^2$ to get confidence levels of 68.27%, 90%, 95%, 99%, 99.73% C.L.

In the graphs shown in Figure (5.6), Figure (5.7), and Figure (5.8), we can see that we got interesting results for the new set of data:

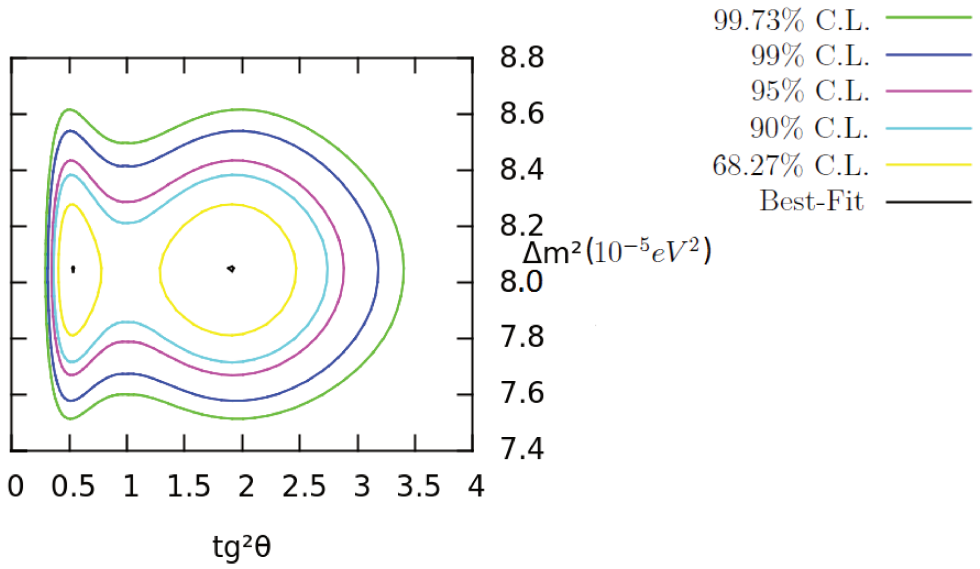

Figure 5.6: Confidence Level Curves for $\tan^2(\theta)$ and Δm^2 made with data from the simulation of our model of oscillation with decoherence considering the new data from reference [11]. The curves correspond to 68.27%, 90%, 95%, 99% and 99.73% C.L.

In the graphs of Figure (5.7) and Figure (5.8), made using the new data, we can see that $\gamma = 0$ is excluded in 68.27% C.L., a result which is different from what was obtained by Lisi et al [14].

In their work, they consider a joint analisis of KamLAND and solar neutrinos, and since it was published in 2007, it doesn't consider the most recent set of data, which is the one [11] we used to get our results.

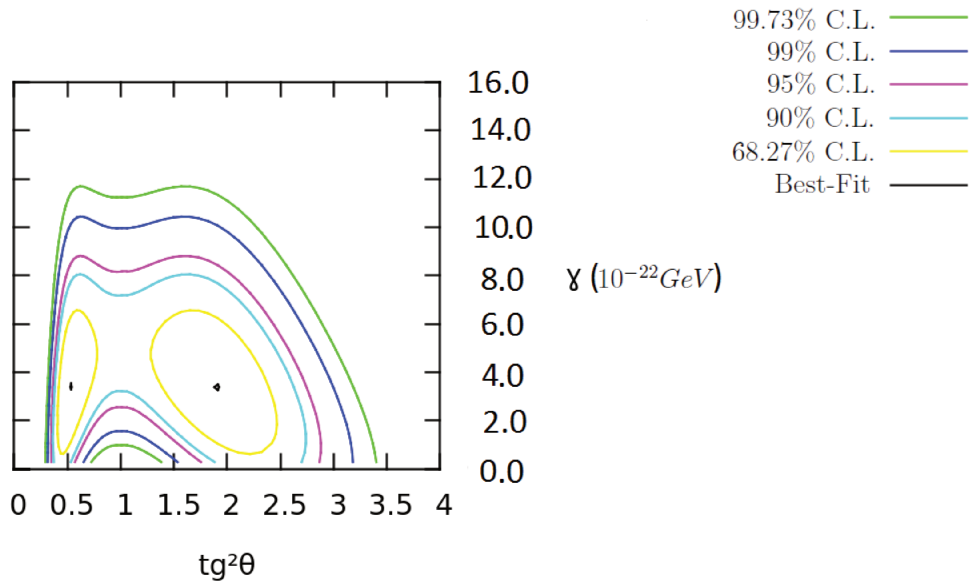

Figure 5.7: Confidence Level Curves for $\tan^2(\theta)$ and γ made with data from the simulation of our model of oscillation with decoherence considering the new data from reference [11]. The curves correspond to 68.27%, 90%, 95%, 99% and 99.73% C.L.

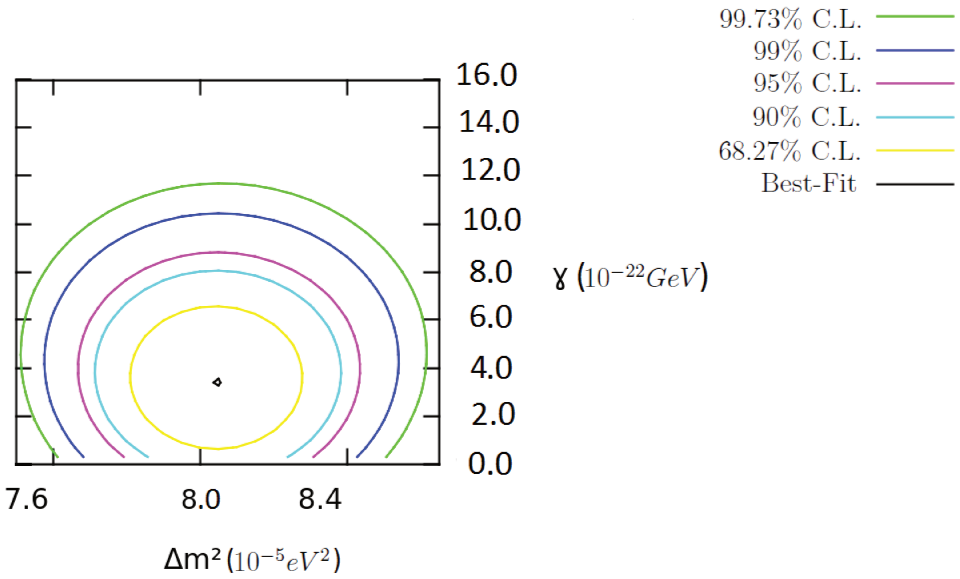

Figure 5.8: Confidence Level Curves for Δm^2 and γ made with data from the simulation of our model of oscillation with decoherence considering the new data from reference [11]. The curves correspond to 68.27%, 90%, 95%, 99% and 99.73% C.L.

Using the confidence level curves, we also obtained the limits for the three free parameters, which are shown in Table (5.7).

68.27% C.L.	$(7.80 < \Delta m^2 < 8.28)10^{-5}eV^2$	$0.40 < \tan^2(\theta) < 0.79$ $1.29 < \tan^2(\theta) < 2.47$	$(0.60 < \gamma < 6.59)10^{-22}GeV$
90% C.L.	$(7.71 < \Delta m^2 < 8.38)10^{-5}eV^2$	$0.37 < \tan^2(\theta) < 2.75$	$(0 < \gamma < 8.10)10^{-22}GeV$
95% C.L.	$(7.67 < \Delta m^2 < 8.44)10^{-5}eV^2$	$0.34 < \tan^2(\theta) < 2.88$	$(0 < \gamma < 8.85)10^{-22}GeV$
99% C.L.	$(7.57 < \Delta m^2 < 8.54)10^{-5}eV^2$	$0.31 < \tan^2(\theta) < 3.18$	$(0 < \gamma < 1.05)10^{-21}GeV$
99.73% C.L.	$(7.51 < \Delta m^2 < 8.62)10^{-5}eV^2$	$0.29 < \tan^2(\theta) < 3.41$	$(0 < \gamma < 1.17)10^{-21}GeV$

Table 5.7: Parameter's Limits for Oscillation with Decoherence Case 1: New Data

In order to visualize the effect of the inclusion of decoherence in our study of neutrino oscillations, we can reproduce an important graph originally presented by the KamLAND Collaboration.

The graph from Figure (5.9) was obtained in reference [11], the same one we used to get the new data, and it is an important graph since it shows directly the oscillation pattern.

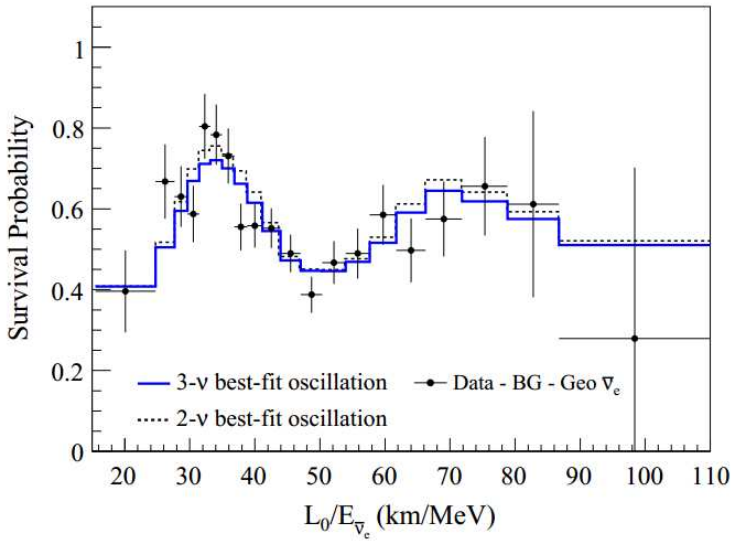

Figure 5.9: Original Graph From KamLAND Collaboration [11]

Using the results of the best-fit values for the neutrino oscillation parameters, we made two versions of the graph that shows the survival probability *versus* L_0/E. The first one, in Figure (5.10), considers $\gamma = 0$, and the second one, in figure (5.11), uses the best-fit value for γ.

In the original graph, Figure (5.9), we see that, even though most of the error bars of the experimental data points reach the best-fit oscillation curves, a few points still allow a different theoretical prediction.

Considering the first curve made from the results of our simulation setting $\gamma = 0$, Figure (5.10), we see that it is very similar to the original one, which is another indication that our original program deserves confidence.

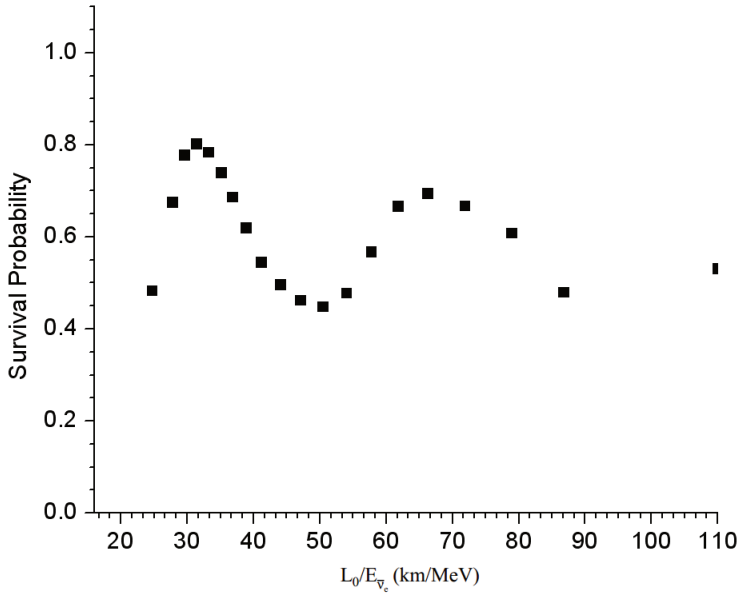

Figure 5.10: Graph showing the oscillation pattern, made with data from the simulation for oscillation without decoherence considering best-fit values of $\Delta m^2 = 8.05 \times 10^{-5} eV^2$ and $\tan^2(\theta) = 0.44$ and setting $\gamma = 0$

In the second curve, in Figure (5.11), we see that the inclusion of decoherence causes a damping on the oscillation pattern, as we already expected from our theoretical predictions. We can also see that this damping isn't too strong, because if we compare the size of the error bars of the original graph with the oscillation with decoherence curve, we can see that it is still a possible curve to fit the data from KamLAND.

Figure (5.12) shows the merging between Figure (5.10) and Figure (5.11), and allos us to see clearly the damping effect.

The Figure (5.13) is the result of merging the original graph and the graph we made for oscillation with decoherence, where the points in red represent our fit of the data.

In Figure (5.13) we can see that the fit of the data made from our model of oscillation with decoherence Case 1 is a good fit of the data, showing a visual confirmation of the analysis provided by the χ^2 Test.

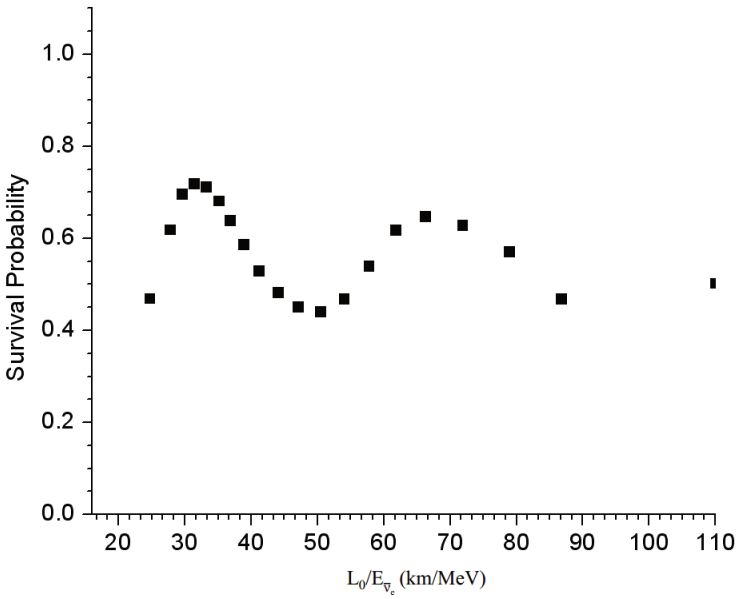

Figure 5.11: Graph showing the oscillation pattern, made with data from the simulation of our model for oscillation with decoherence considering best-fit values of the three parameters:$\Delta m^2 = 8.05 \times 10^{-5} eV^2$, $\tan^2(\theta) = 0.54$ and $\gamma = 3.15 \times 10^{-22} GeV$

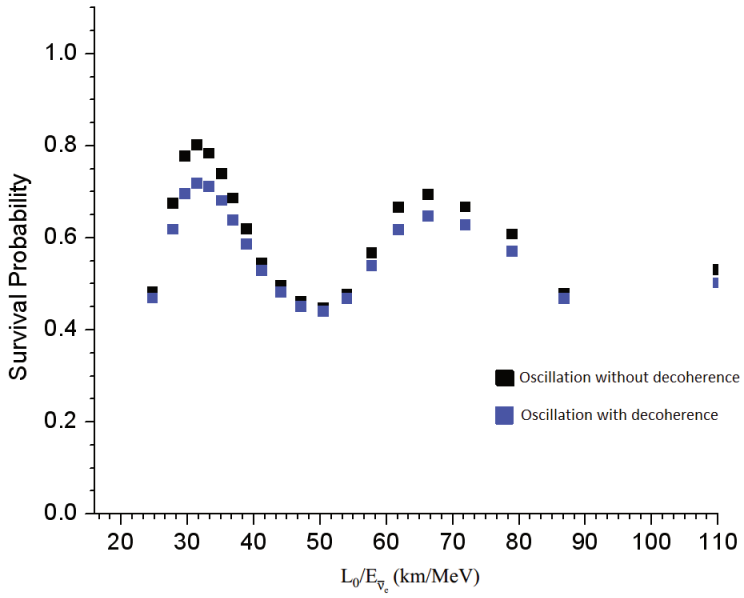

Figure 5.12: Merging between graph showing simulation results for oscillation without decoherence, with $\Delta m^2 = 8.05 \times 10^{-5} eV^2$ and $\tan^2(\theta) = 0.44$ and $\gamma = 0$(data in black) and graph showing simulation results for oscillation with decoherence, using $\Delta m^2 = 8.05 \times 10^{-5} eV^2$, $\tan^2(\theta) = 0.54$ and $\gamma = 3.15 \times 10^{-22} GeV$ (data in blue), where we can see the damping effect on the oscillation pattern.

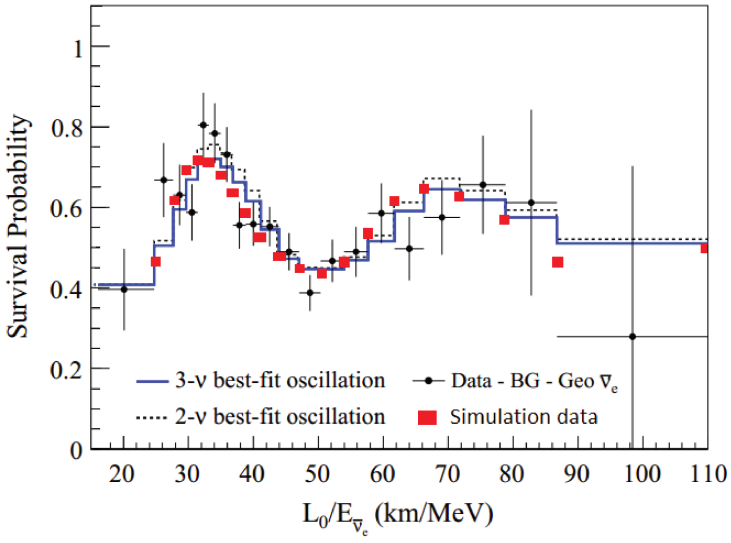

Figure 5.13: Merging of original KamLAND graph [11] and graph made with data from the simulation of our model for oscillation with decoherence (data in red) considering best-fit values of the three parameters:$\Delta m^2 = 8.05 \times 10^{-5} eV^2$, $\tan^2(\theta) = 0.54$ and $\gamma = 3.15 \times 10^{-22} GeV$

Chapter 6

Conclusions and Future Perspectives

In this work, we treated the appearence of the decoherence effect on neutrino oscillations in a phenomenological approach, studying first Quantum Open Systems in general, and then aplying the results to the case of neutrino oscillation in two families, since it is one of the models used in the analysis of KamLAND data.

In Chapter 2 we studied the quantum superposition principle and the measurement problem, and we considered the possibility of dealing with the measurement problem by making the measurement instrument have a coupling with the system of interest, working with an example of how this could be achieved using Quantum Mechanics concepts.

We then proceeded, presenting the aspects of the theory of Quantum Open Systems that would be necessary to the study of the neutrino system. And in order to do that, we first introduced the formalism of density matrix, which is used through this whole dissertation. In the context of a global system, we defined the Partial Trace, an operation that allow us to get information from the subsystem of interest as if it were isolated. Using the partial trace, and with the assumption that the coupling between the subsystem of interest and the enviroment is weak enough, we derived an equation that defines the time evolution of density operator of the subsystem of interest, the Lindblad - Kossakowski equation.

Chapter 3 was devoted to the study of neutrino oscillations, initially showing an example how we would treat the usual model of vaccum neutrino oscillations in two families using the density matrix formalism, and then applying the Lindblad - Kossakowski equation obtained in Chapter 2 to develop two different models for the neutrino oscillations considering a coupling with the enviroment, where we saw the appearence of the decoherence effect in both models, and for the Case 2 we saw a different flavor convertion mechanism, independent of quantum superpositions.

In Chapter 4 we did a brief analysis of neutrino experiments and presented some information about KamLAND. We also showed the model used for the χ^2 Test and details of the method used to confront our model of neutrino oscillation with decoherence Case 1 with the data from KamLAND.

We finally presented the results of the analysis in Chapter 5, where we saw that the program used for the data analysis provided a good reproduction of the KamLAND results for the usual neutrino oscillation case. The results of the best-fit for this test are presented in Table (5.1) and the confidence level curves can be seen in Figure (5.1). The good results of our test allowed us to

begin the simulations for the probability Case 1.

Using data from reference [10] we obtained a good agreement with experimental data, and found the result that we had a best-fit with $\gamma \neq 0$, a result that suggested that including decoherence in the theory of neutrino oscillations improved the description of the phenomenon. The best-fit results for this set of data are in Table (5.3). We also presented the confidence level curves for this set of data in figures (5.3), (5.4) and (5.5), and we used these figures to find limits for Δm^2, $\tan^2(\theta)$ and γ, which are presented in Table (5.4).

But the most interesting results were obtained when we considered the most recent set of data, provided by reference [11], where the number of events were presented for 20 bins. Comparing the value of χ^2_{min} with the number of degrees of freedom, we saw that including the third parameter, γ, improved considerably the fit of the data. With $\gamma = 0$ we obtained $\chi^2_{min} = 24.88$, and for γ as a free parameter (hence 20 experimental points and 3 parameters) we obtained $\chi^2_{min} = 21.36$, a 3.52 unit decrease. These results are sumarized in tables (5.5) and (5.6). We also found a best-fit value with $\gamma \neq 0$, and the graphs of the confidence level curves showed that a solution with $\gamma = 0$ was excluded with 68.27% C.L., as we can see from Figures (5.7) and (5.8) a different result from what is found in the literature.

To support the results of our analysis, giving a more visual way of evaluating the results, we reproduced an important graph originally presented by the KamLAND Collaboration, that can be ssen in Figure (5.9), which showed the survival probability *versus* L_0/E, and is a graph that shows clearly the oscillation pattern for the neutrinos.

We made two reproductions, the first one considering $\gamma = 0$ is presented in Figure (5.10), and provided another confirmation that our original program was a good tool for the KamLAND data analysis, and the second one, in Figure (5.11) was made using the best-fit values for the case of γ as a free parameter. The second graph clearly showed the dumping generated by the decoherence effect, when we compared with Figure (5.10).

By merging the original graph with our reproduction of the graph, which mas made using the best-fit values obtained in our simulation, we saw that our model provided a fit of the data which was indeed in agreement with the experiment uncertainties, as can be seen in Figure (5.12). So we have another evidence that our model is a realistic one.

We also determined limits for the three parameters, Δm^2, $\tan^2(\theta)$ and γ, in 68.27%, 90%, 95%, 99%, 99.73% C.L.. The limits are presented in Table (5.7), and were determined based on the confidence level curves made from this most recent set of data [11], and are in Figures (5.6), (5.7), and (5.8).

Therefore, in this work we saw that, even though the usual model for neutrino oscillations provides a good fit for the experimental data, our anlysis supports the idea that including the decoherence effect can improve this fit, which can be seen as an evidence that treating the system of interest in a coupling with the enviroment may be a more realistic approach to the study of quantum systems.

To proceed with our studies, several things can be made. We can use other models of oscillation with decoherence, for example the Case 2 presented in Chapter 3, or even other options that may come from other possible forms of the dissipative matrix.

But, still considering our model Case 1, we could include $\theta_1 3$ in the analysis, since we know that KamLAND has sensitivity for this parameter. We could also include in γ a dependence with the

energy, as done in reference [14], and do a detailed study of the inclusion of solar neutrinos in this analysis, since solar neutrino experiments are usually related to the KamLAND. There is also the possibility of doing a complete analysis for three families, including data from other experiments.

As we can see, there are a lot of possible studies to be made in this area, and since it is related to very fundamental concepts, these studies can help in the understanding of important aspects of physics.

References

[1] R.L.N. Oliveira *Análise Fenomenológica da Descoerência na Oscilação de Neutrinos* 2007: Dissertação (Mestrado em Física) – Curso de Pós-Graduação em Física, UNICAMP, São Paulo

[2] H. P. Breuer, F. Petruccione, *The Theory of Open Quantum Systems*, Lect. Notes Phys. (Oxford University Press, Oxford, 2002)

[3] E. B. Davies, Markovian master equations. *Commun. Phys.*, v. 39, p. 91, 1974.

[4] E. Joos, *et al.*, *Decoherence and the Appearance of Classical World in Quantum Theory*, 2ed. Springer, New York, (2003).

[5] C. W. Kim, C. Giunti, *Fundamentals of Neutrino Physics and Astrophysics.* 1ed. Oxford University Press, Oxford, (2007).

[6] M.C. Gonzalez-Garcia, M. Maltoni, *"Phenomenology with Massive Neutrinos,"* Phys. Rept. **460**, 1 (2008) [arXiv:0704.1800 [hep-ph]].

[7] Toshiyuki Iwamoto. *Measurement of Reactor Anti-Neutrino Disappearance in KamLAND.* Graduate School of Science, Tohoku University, Feb 2003.

[8] S. Abe, S. Enomoto, K. Furuno, *et. al. Production of radioactive isotopes through cosmic muon spallation in KamLAND.*

[9] The KamLAND Collaboration, "Precision Measurement of Neutrino Oscillation Parameters with KamLAND," Phys. Rev. Lett. **100**, 221803 (2008) [arXiv:0801.4589 [hep-ex]].

[10] Shimizu I., 2007 *"KamLAND (Anti-neutrino status)"* Slide in The 10th International Conference on Topics in Astroparticle and Underground Physics, Tokohu Univ.

[11] A. Gando *et al.* [KamLAND Collaboration], "Constraints on θ_{13} from A Three-Flavor Oscillation Analysis of Reactor Antineutrinos at KamLAND," Phys. Rev. D **83**, 052002 (2011) [arXiv:1009.4771 [hep-ex]].

[12] Bevington P.R., Robinson D. K - *Data Reduction and Error Analysis For The Physical Sciences.* New York: 3e. McGraw-Hill (2003).

[13] J. Beringer et al. (Particle Data Group), Phys. Rev. D86, 010001 (2012)

[14] E. Lisi et al,Probing non-standard decoherence effects with solar and KamLAND neutrinos. *Phys.Rev.D*,76:033006,(2007).

[15] R.L.N. Oliveira, *Dissipação Quântica em Oscilações de Neutrinos*, Tese (Doutorado em Física) – Curso de Pós Graduação em Física, UNICAMP, São Paulo, (2012).

[16] J. Ellis, *et al.*, Search for violations of quantum mechanics, *Nucl. Phys. B*, 241, 381, (1984).

[17] D. Griffiths, *Introduction to Elementary Particles*, John Wiley, (1987).

[18] M. C. Gonzalez-Garcia, M. Maltoni and J. Salvado, "Updated global fit to three neutrino mixing: status of the hints of $\theta_{13} > 0$," JHEP **1004**, 056 (2010) [arXiv:1001.4524 [hep-ph]].

[19] F. Melo, Descoerência na Propagação de Neutrinos. Dissertação (Mestrado em Física) - Curso de Pós-Graduação em Física, UNICAMP São Paulo, (2003).

[20] KamLAND Collaboration, K. Eguchi *et al.*, First Results from KamLAND: Evidence for Reactor Antineutrino Disappearance,*Phys. Rev. Lett.*, 90, 021802, (2003).

[21] SK Collaboration, Y. Fukuda et al., Evidence for Oscillation of Atmospheric Neutrinos, *Phys. Rev. Lett.*, 81, 1562, (1998).

[22] Homestake Collaboration, T. B. Cleveland *et al.*, Measurement of the Solar Electron Neutrino Flux with the Homestake Chlorine Detector, *Astrophys. J.*, 496, 505, (2003).

[23] P. A. M. Dirac, *The Principles of Quantum Mechanics.* Oxford: Clarendon Press,(1947).

[24] A. Einstein, B. Podolsky, N. Rosen, Can quantum-mechanical description of physical reality be considered complete. *Phys. Rev.*, v. 47, p. 777, (1935).

[25] J. S. Bell, On the eintein podolsky rosen paradox. *Physics*, v. 1, p. 195, (1964).

[26] R. Omnès, A new interpretation of quantum mechanics and its concequences in epistemology. *Found. Phys.*, v. 25, p. 605, (1995).

[27] G. C. Ghirardi, A. Rimini, T. Weber, Unified dynamics for microscopic and macroscopic systems. *Phys. Rev. D*, v. 34, p. 470, (1986).

[28] I. C. Percival, Localisation of wide open quantum systems. *J. Phys. A*, v. 24, p. 1003, (1994).

[29] R. J. Cook, What are quantum jumps. *Physica Scripta T*, v. 21, p. 49, (1988).

[30] C. Cohen-Tannoudji, *et al., Quantum Mechanics*, V.I, Hermann, Paris, (1977).

[31] T. Schwetz, "Variations on KamLAND: Likelihood analysis and frequentist confidence regions," Phys. Lett. B **577**, 120 (2003) [hep-ph/0308003].

[32] R. L. N. Oliveira, M. M. Guzzo, Quantum dissipation in vacuum neutrino oscillation. *Eur. Phys. Jour. C*, v. 69, p. 493, (2010).

[33] R. L. N. Oliveira, M. M. Guzzo, Dissipation and θ_{13} in Neutrino Oscillations. *Eur. Phys. Jour. C*, v. 73, p. 2434, (2013).

[34] R. L. N. Oliveira, M. M. Guzzo, and P. C. de Holanda, "Quantum Dissipation and CP Violation in MINOS," *Phys. Rev. D* **89**, 053002 (2014). arXiv:1401.0033v4 [hep-ph]